

The INTEGRAL IBIS/ISGRI

Standard Data Analysis

Andrea Goldwurm & Aleksandra Gros

Service d' Astrophysique – CEA Saclay, France

Content

General presentation of the standard procedures implemented in the ISDC OSA pipeline for the analysis of the IBIS/ISGRI data.

Contributions, references

Coded mask imaging

The IBIS/ISGRI telescope, data format

Instrumental effects: noisy pixels, charge loss

Energy correction

Image binning and efficiency computation

Background correction

Imaging: decoding, cleaning

Imaging: SPSF characteristics and Point Source Location

Imaging: mosaics

Spectral extraction

Timing analysis

Contributions

The IBIS/ISGRI scientific data analysis s/w defined and developed to be implemented in the ISDC system as Instrument Specific SoftWare (ISSW) is the result of the work of a large team in the IBIS institutes and in ISDC (1999-2004).

Main contributions were provide by

ISSW Definition and Development:

S. Chazalmartin, P. David, A. Goldwurm, A. Gros, P. Laurent, A. Sauvageon
(SAp - Saclay)

L. Lerusse, N. Produit, (ISDC – Versoix)

Instrument responses, bkg and calibration files, algorithms:

F. Lebrun, P. Laurent, R. Terrier (SAp – Saclay)

Tests and control of performances:

G. Belanger, M. Cadolle Bel, M. Falanga, M. Forot, P. Goldoni, S. Kuzentsov, M. Renaud, J. Rodriguez (SAp – Saclay)

L. Foschini (IASF – Bologna)

Del Santo, L. Natalucci (IASF – Roma)

Others ... at ISDC – Versoix

References

Coded mask imaging:

**Fenimore & Cannon, 1979 & 1981, App. Opt.
Gottesman & Fenimore, 1989, App. Opt.**

Data analysis for the SIGMA/GRANAT experiment:

**Goldwurm, 1995, Exp. Astr.
Bouchet et al., 2001, Ap.J.**

IBIS data analysis concepts:

**Goldwurm et al., 2001, ESA - SP
Goldwurm et al., 2003, A&A, 411
Gros et al., 2003, A&A, 411**

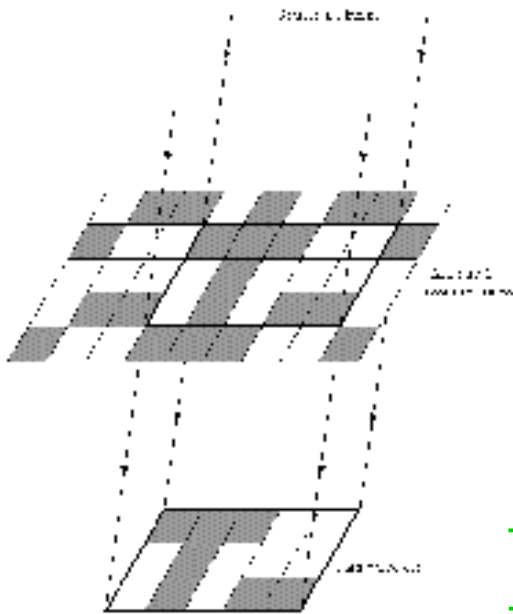
IBIS/ISGRI in-flight calibrations, responses, performances:

**Lebrun et al. 2003 and Terrier et al., 2003, A&A, 411
Sauvageon et al., 2003, IBIS Report
Natalucci et al., 2004, IBIS Report**

IBIS data analysis manual:

**Chernyakova, 2004, IBIS Data Analysis Manual
(ISDC documentation)**

Coded Mask Imaging : Concept



Coded Aperture Systems employ a **mask** of opaque and transparent elements to modulate sky radiation before it is recorded by a **position sensitive detector**. Sources project patterns of the mask on the detector (pinhole camera concept), and an image can then be reconstructed by correlation with the known mask.

To reconstruct a sky image the **mask pattern** must be such that

- the projected shadow by any given source must be unique
- the match between shifted patterns must be as poorest as possible

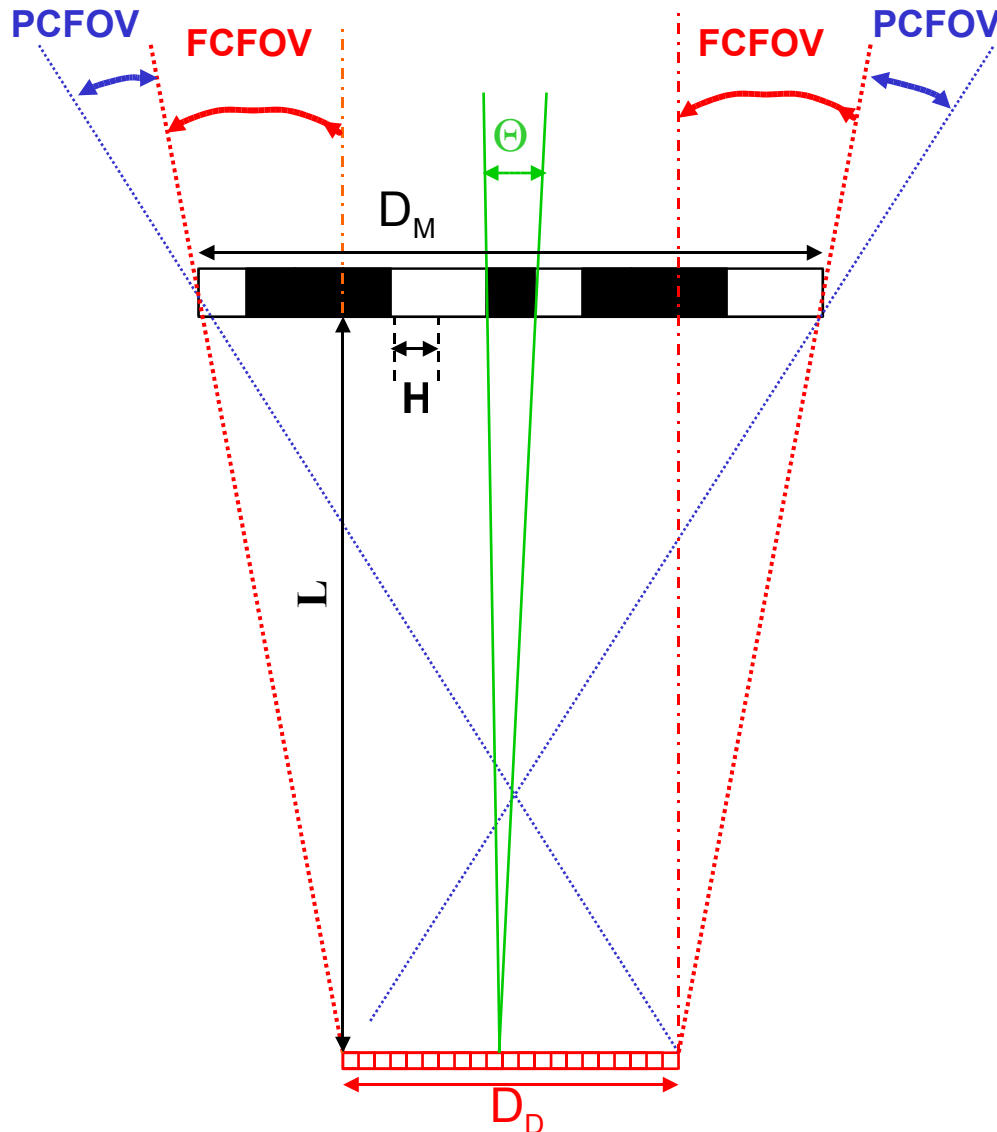
Advantages :

- Angular resolution is given by SIZE of elements and by mask-detector DISTANCE and large Field of View (FOV) can be obtained.
- Sensitivity depends on the NUMBER of (open) mask elements
- Background is measured simultaneously to the source fluxes

Problems :

- Not-direct imaging, decoding needed (slow)
- *Collective / Statistical* imaging, not event by event.

Coded Mask Imaging : Parameters



Mask

Opaque/transparent elements

Element size constant = H

Distance from detector = L

Mask dimension = D_M

Position Sensitive Detector

Dimension $D_D \leq$ mask dim D_M

Pixels size \leq mask element size

Two Fields of View

Fully Coded (sens. \sim const.)

$$\Theta_{FC} = \arctg ((D_M - D_D) / L)$$

Partially Coded (decr. sens.)

$$\Theta_{PC} = \arctg ((D_M + D_D) / L)$$

Angular Resolution

$$\Theta = \arctg (H/L)$$

Coded Mask Imaging : Coding & Decoding

Source flux (S) is modulated by mask (M) before being recorded by a position sensitive detector, the resulting image (D) is, if B is background :

$$D = S * M + B$$

If it exists G such that $G * M = \delta$ (= delta function), reconstructed sky S' is

$$S' = D * G = S * M * G - B * G = S * \delta - B * G = S - B * G$$

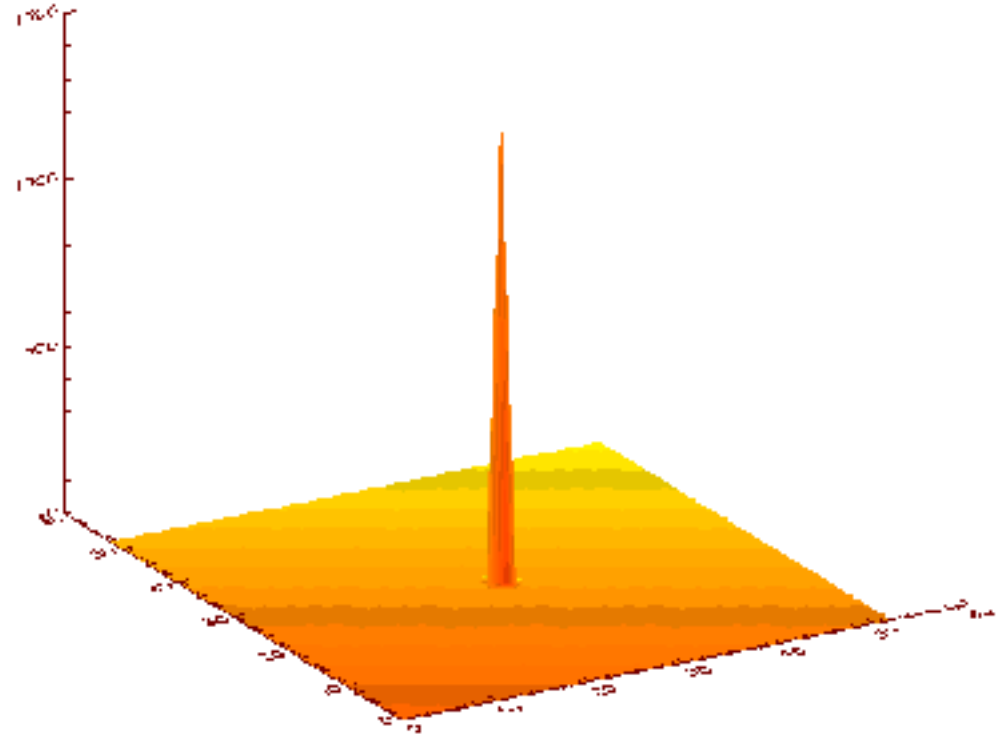
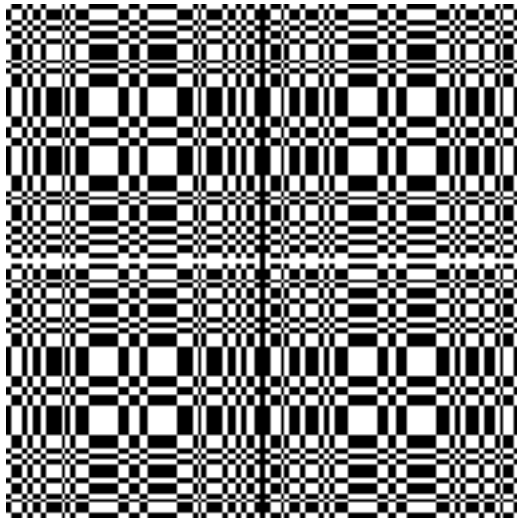
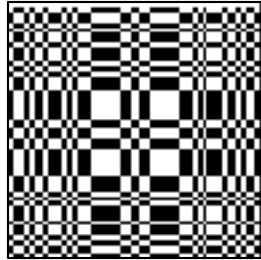
S' = S apart from the background term B * G, a constant level if B uniform.

Such array G exists for **Uniformly Redundant Arrays (URA)**, built using **cyclic different sets**, binary sets with a **cyclic autocorrelation function** = δ
For URA $G = 2M - 1$ (-1 associated to opaque, +1 to transparent elem.).

Essential properties for γ -ray imaging :

- **Angular resolution** increases by varying hole size or mask-detector distance without losing sensitive area (unlike a pinhole camera)
- Simultaneous **measure** of sources and background
- Projected source pattern is **unique** and provide **flat side lobes response**
- URAs have half open and half close elements : **best S/N condition**

Coded Mask Imaging : Optimum System



- A 53 x 53 MURA (Modified URA) Basic Pattern
- The Replicated (2 times - 1) Basic Pattern
- Their cross-correlation : a delta function, the Point Spread Function in the FCFOV

Coded Mask Imaging : Errors and Noise

Statistical errors

URA (as Hadamard or other optimum masks) provide best statistical error since $G = +1$ or -1 . Assuming Poissonian statistics of detector count rates:

$$V(S') = V(D * G) = G^2 * V(D) = V(D) = \text{Total number of detector counts } C$$

Source signal to noise ratio (S/N) for a measured source intensity I_s is then

$$S / N = I_s / V^{1/2} = I_s / (C)^{1/2}$$

However any deviation from optimum system induce systematic errors.

Systematic errors

The worse are those which **depend on the background**.

Condition B = uniform over detector plane is usually not verified.

In this case the decoding procedure magnifies the variations.

=> need to correct the non-uniform background spatial distribution

Other source of systematic noise is the **non perfect coding** (side lobes in the PSF) due to non-perfect system (dead zones, geometrical effect, etc.).

Coding noise is proportional to source flux.

In the PCFOV, URA mask properties are not satisfied so there the PSF will have side lobes (8 main ghost peaks + distributed coding noise).

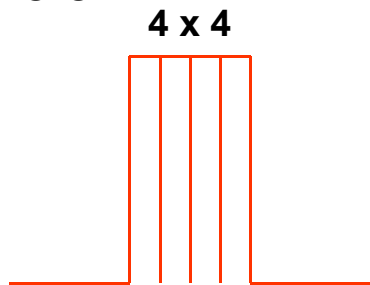
Coded Mask Imaging : Sampling

Unless the source is right in the middle of a sky pixels the reconstructed peak will be shared by different pixels and there is a loss of efficiency (we will call this imaging loss). You can perform a SPSF-fit (see below) to recover part of the peak height but a certain loss is inevitable.

To reduce this loss the detector must have spatial resolution better than the mask element size. Detector pixels (resolution) over-sample the mask elements ($n \times n$). In this case the decoding can take the form of

Fine cross-correlation: G and S elements are also sampled in $n \times n$ pixels and the correlation run on all them

Delta-decoding : same but $G=2M-1$ in only 1 pix out of the $n \times n$, =0 elsewhere



Decoding Array G

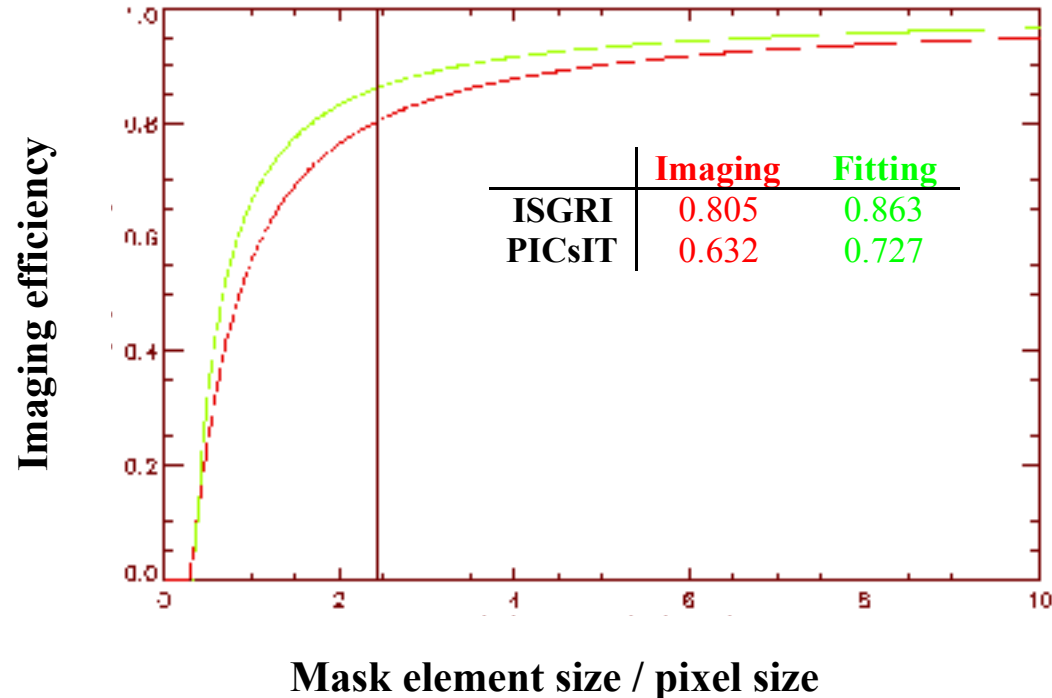
Fine C-C

-1	-1	-1	-1	1	1	1	1
-1	-1	-1	-1	1	1	1	1
-1	-1	-1	-1	1	1	1	1
-1	-1	-1	-1	1	1	1	1
1	1	1	1	-1	-1	-1	-1
1	1	1	1	-1	-1	-1	-1
1	1	1	1	-1	-1	-1	-1
1	1	1	1	-1	-1	-1	-1

Delta-Dec

0	0	0	0	0	0	0	0
0	-1	0	0	0	1	0	0
0	0	0	0	0	0	0	0
0	0	0	0	0	0	0	0
0	0	0	0	0	0	0	0
0	1	0	0	0	-1	0	0
0	0	0	0	0	0	0	0
0	0	0	0	0	0	0	0

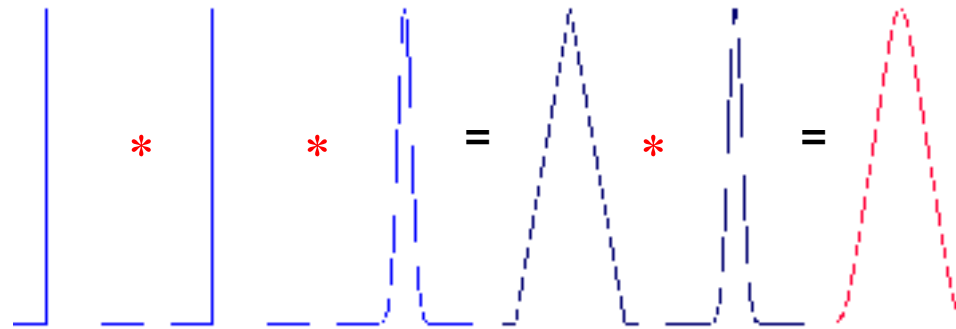
Coded Mask Imaging : Imaging Efficiency Loss



Expected average values of imaging efficiency due to discrete binning as function of the ratio (r) between mask element – pixel sizes for simple fine cross-correlation and for SPSF fitting. Values expected for both IBIS detectors ISGRI ($r=2.4$) and PICSIT ($r=1.2$) pixel to mask element size ratios.

Coded Mask Imaging : the SPSF

The final **System Point Spread Function** (after decoding) of a optimum coded mask system is independent of position in FCFOV and given by the convolution of a block function (describing the peak of the delta function) with a function describing the kind of decoding applied and then with a function which describes the detector spatial resolution. For example for fine cross-correlation decoding (4 pix per mask el.) and a Gaussian Detector-PSF with $\sigma_d = 0.5$ pix the SPSF looks like :



Chi-square fit of the analytical SPSF with a decoded image sector is then employed to obtain fine source location estimate and position error.

Point Source Location Error depends on source signal to noise (SNR) as

$$\text{PSLE} : 1 / \text{SNR}$$

Coded Mask Imaging : Decoding in PCFOV

Discrete correlation to reconstruct sky image and variance in FCFOV is written using D_{kl} , M_{kl} , S_{ij} , $G_{kl} = 2 M_{kl} - 1$, array elements as

$$S_{ij} = \sum D_{kl} G_{i+k,j+l}$$
$$V_{ij} = \sum D_{kl} (G_{i+k,j+l})^2$$

To extend decoding procedure in PCFOV we can use G^+ and G^- arrays defined as $G^+ = M$, $G^- = 1 - M$, padded with 0 outside the mask :

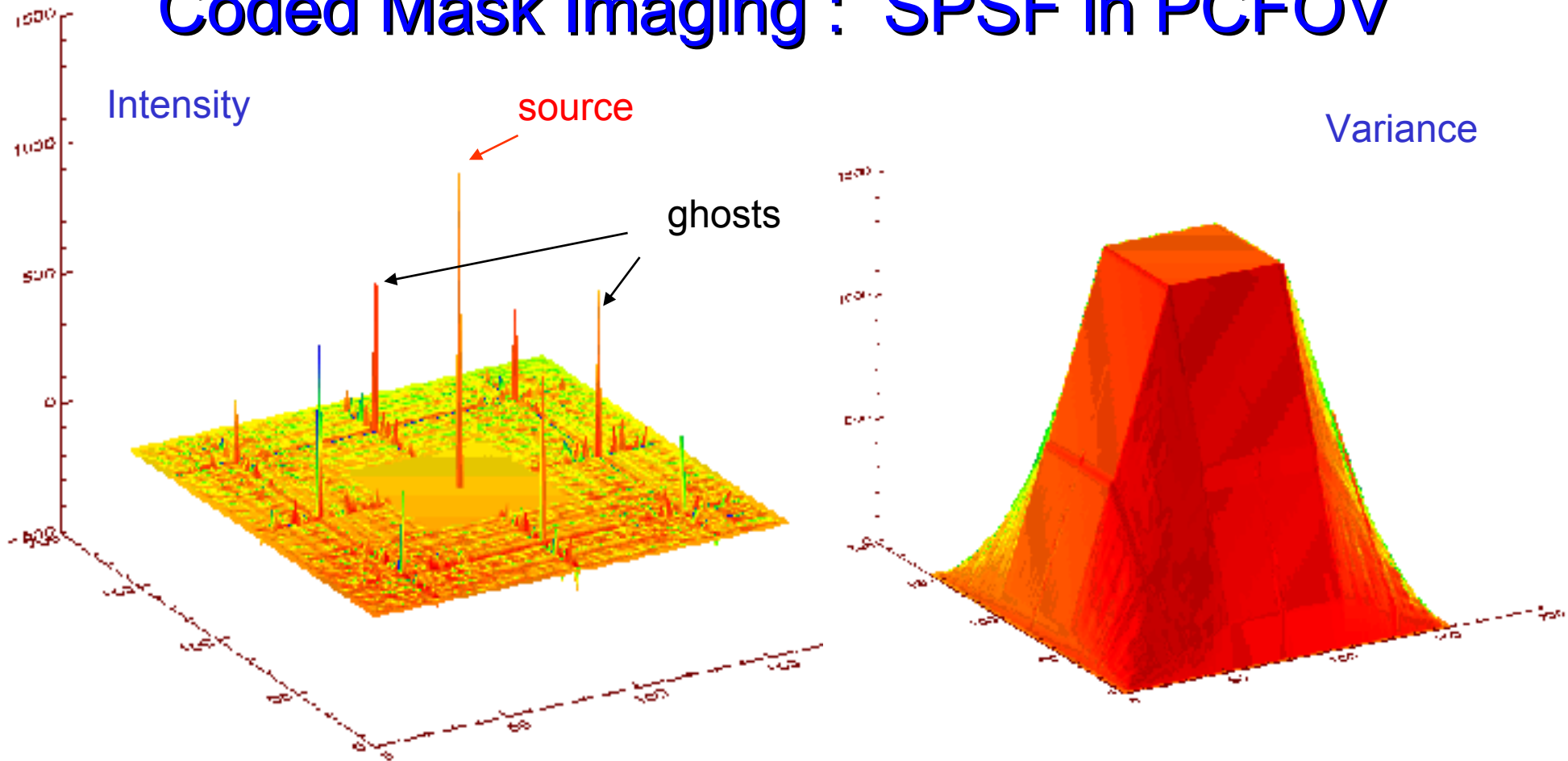
$$S_{ij} = \sum W_{kl} D_{kl} G^+_{i+k,j+l} - b_{ij} \sum W_{kl} D_{kl} G^-_{i+k,j+l}$$
$$b_{ij} = \sum W_{kl} G^+_{i+k,j+l} / \sum W_{kl} G^-_{i+k,j+l}$$
$$V_{ij} = \sum D_{kl} (W_{kl} G^+_{i+k,j+l})^2 + b_{ij}^2 \sum D_{kl} (W_{kl} G^-_{i+k,j+l})^2$$

Details :

- Weighting array $W_{kl} \neq 1$ can be used to take into account some effects (attitude drifts, IBIS detector dimension > mask pattern, etc.)
- To take into account finite spatial resolution or not exact binning of mask elements (IBIS) G can assume values between +1 and -1
- These operations can be performed in fast way by a combination of

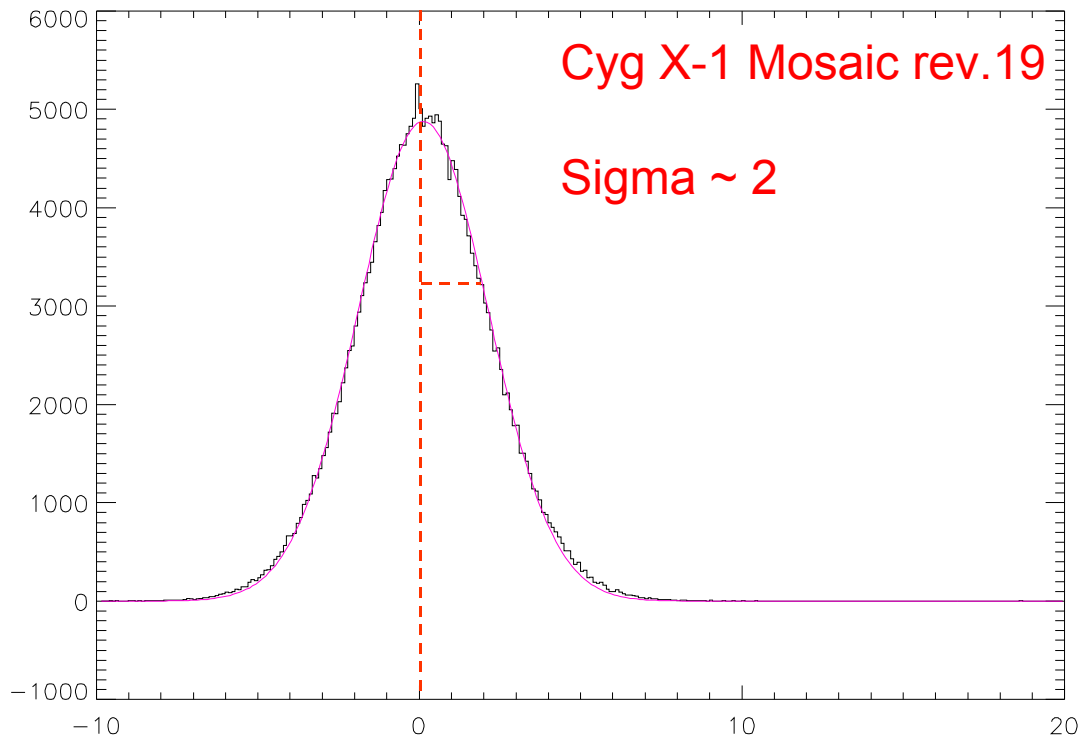
array operations and Discrete Fourier Transforms (DFT)

Coded Mask Imaging : SPSF in PCFOV



- Point Spread Function of the Extended Balance Correlation in FC + PC FOV for a 53 x 53 MURA Optimum System and an on-axis source :
Delta Function in FCFOV + Coding noise in the PCFOV (8 ghosts + noise)
- Variance associated to the reconstructed sky image: constant over the FCFOV decreasing (increasing in relative value) in the PCFOV

Coded Mask Imaging : Significant Excesses



Distribution of Significances

- Distributed as a Gaussian
- Width should be 1
- Measured Width provides a estimate of residual systematic noise

- To search for significant excess in a decoded image, one has to consider that all sky image values are derived from the same set of data
- An excess must be much higher than the canonical 3 sigma to be significant
- For the number of IBIS mask elements an excess (not corresponding to a known source) starts to become significant **for S/N ~ 5 - 6**

The Coded Mask IBIS Telescope

Mask :

53 x 53 MURA basic pattern,
95 x 95 W elem. of size 11.2 x 11.2 mm²
at a distance $L = 3.2$ m from the detector

Positional Detectors :

ISGRI : 128 x 128 pix

PICsIT : 64 x 64 pix bars

Some dead-zones, off pixels

Shielding system, Veto and CU :

Passive (tube, hopper)

Veto Unit : 16 BGO mod

Calibration Unit : ²²Na Source

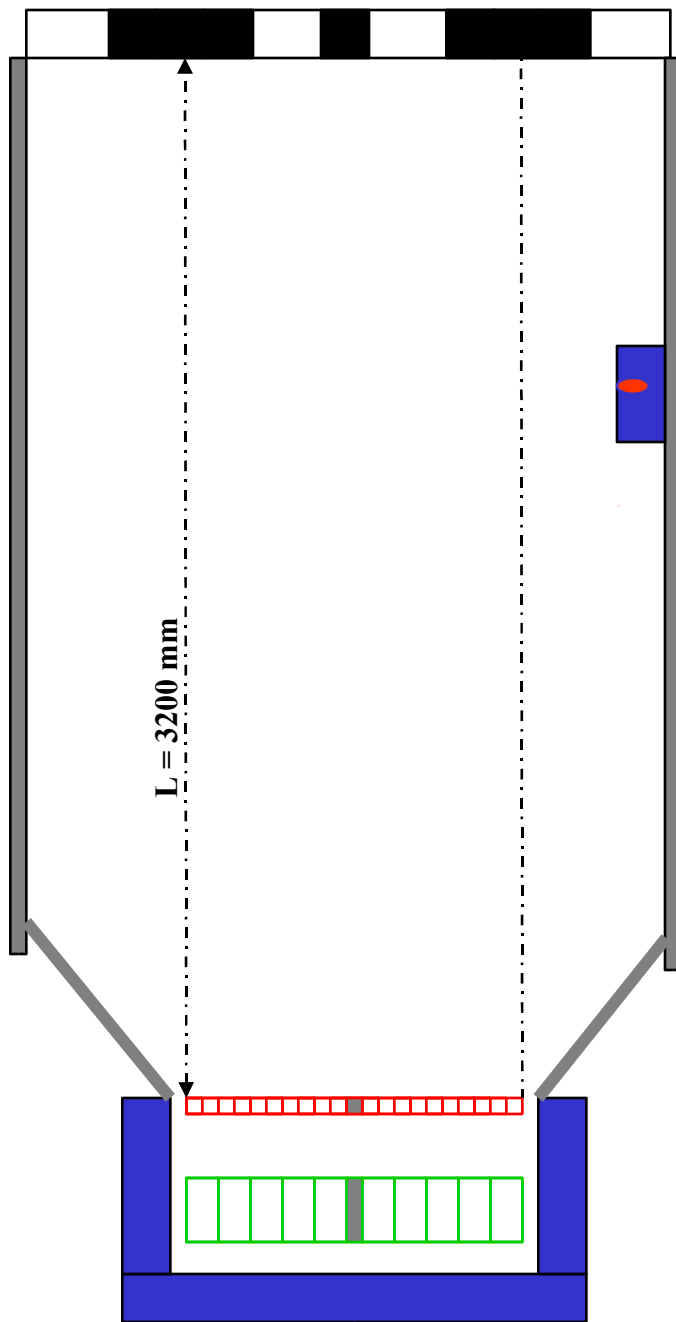
Imaging properties :

FCFOV $9^\circ \times 9^\circ$

FC+PCFOV $29^\circ \times 29^\circ$

Angular Resolution 12'

ISGRI/PICsIT pixels 5' / 10'



IBIS / ISGRI Performances

Energy Band	20 keV-1 MeV
Angular Resolution	12'
FOV at 100% s.	9° x 9°
at 0 sensitivity	29° x 29°
Point Source Location Err.	30'' (S/N~30)
Temporal resolution	60 μ s
	<u>100 keV</u>
Sensitivity (ph cm ⁻² s ⁻¹ keV ⁻¹)	4 10^{-7}
(for 10 ⁶ s, 3 σ , $\Delta E=E$)	1 mCrab
Narrow line sens. (cm ⁻² s ⁻¹)	10 ⁻⁵
Spectral resolution	8 keV

OMC (visible band)

IBIS γ - ray imager

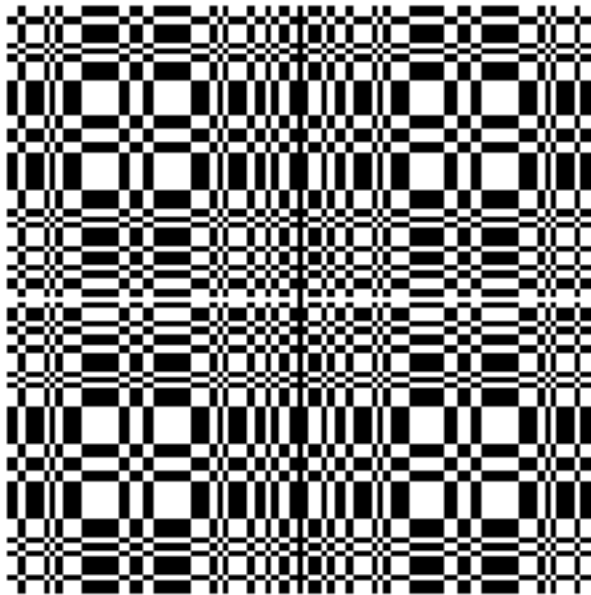
JEM- X (X- ray)

ISGRI camera

SPI γ - ray spectrometer

IBIS Mask, Veto and Calibration

Unit



MASK

MURA basic pattern 53 x 53

Total number of W el. 95 x 95

El. Dimension = 11.2 x 11.2 mm²

El. Thickness = 16 mm

Transparency: 60% @ 20 keV

82% @ 60 keV

Veto system

Anticoincidence system around the 2 detector layers, made of 16 BGO modules viewed by 32 PMT

Calibration Unit

A source of ²²Na which emits two 511 keV photons in opposite directions is placed on the passive shield tube. It is viewed by a BGO+PMT module which detects one of the 511 keV photons. CU tagged events are used to measure 1% gain variations in PICSIT pixels on time scales of few hours

ISGRI : The Soft Gamma-Ray Imager

New-generation gamma-camera of Cadmium Telluride (CdTe), semiconductor with high Z (48-52) working at room temperature.

128 x 128 = 16384 pixels (4 x 4 mm², 2 mm thick) in 8 modules

Energy range : 20 - 1000 keV

Spatial resolution : 4.6 mm (separation of pixel centers)



ISGRI Data in the Telemetry:

- Single-Event List with
Y Z Pha RT t (S1)
- Single event in coincidence
with CU event (calib.) (S2)
- Contexts of the Instrument
(pixels off, thresholds, gains) (CTX)
- House-keepings (HK)
(ratemeters, temperatures,
voltage, pixels status, etc.)

ISGRI specific effects: Charge Loss

Charge-Loss

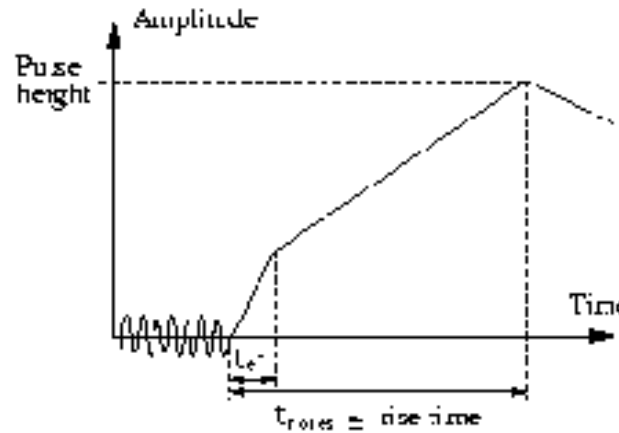
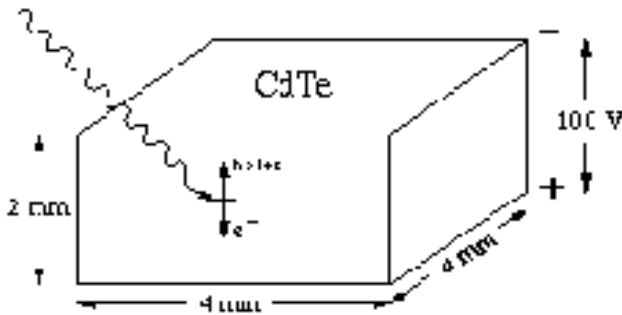
Holes take more time to reach the electrode and a larger charge loss occurs the deeper is the interaction

Rise-Time

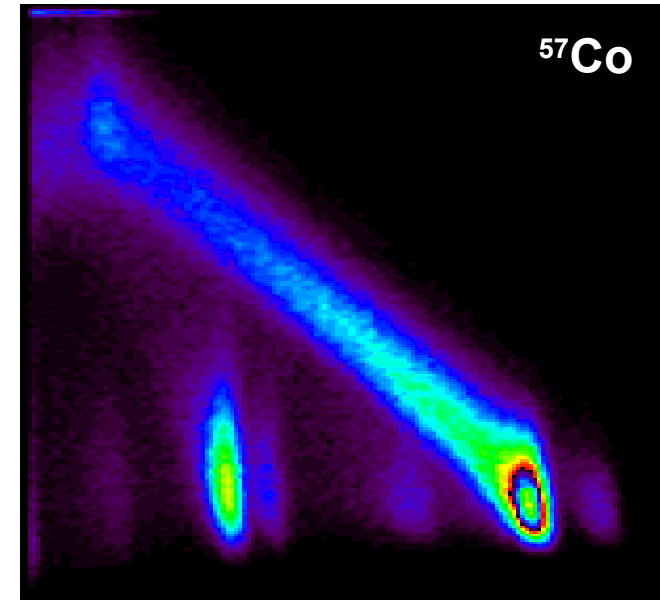
The energy loss is related to the pulse rise time (RT) which is measured and transmitted to ground

Correction

Rise-time can be used to correct the pulse heights (Pha) and compute the deposited energy

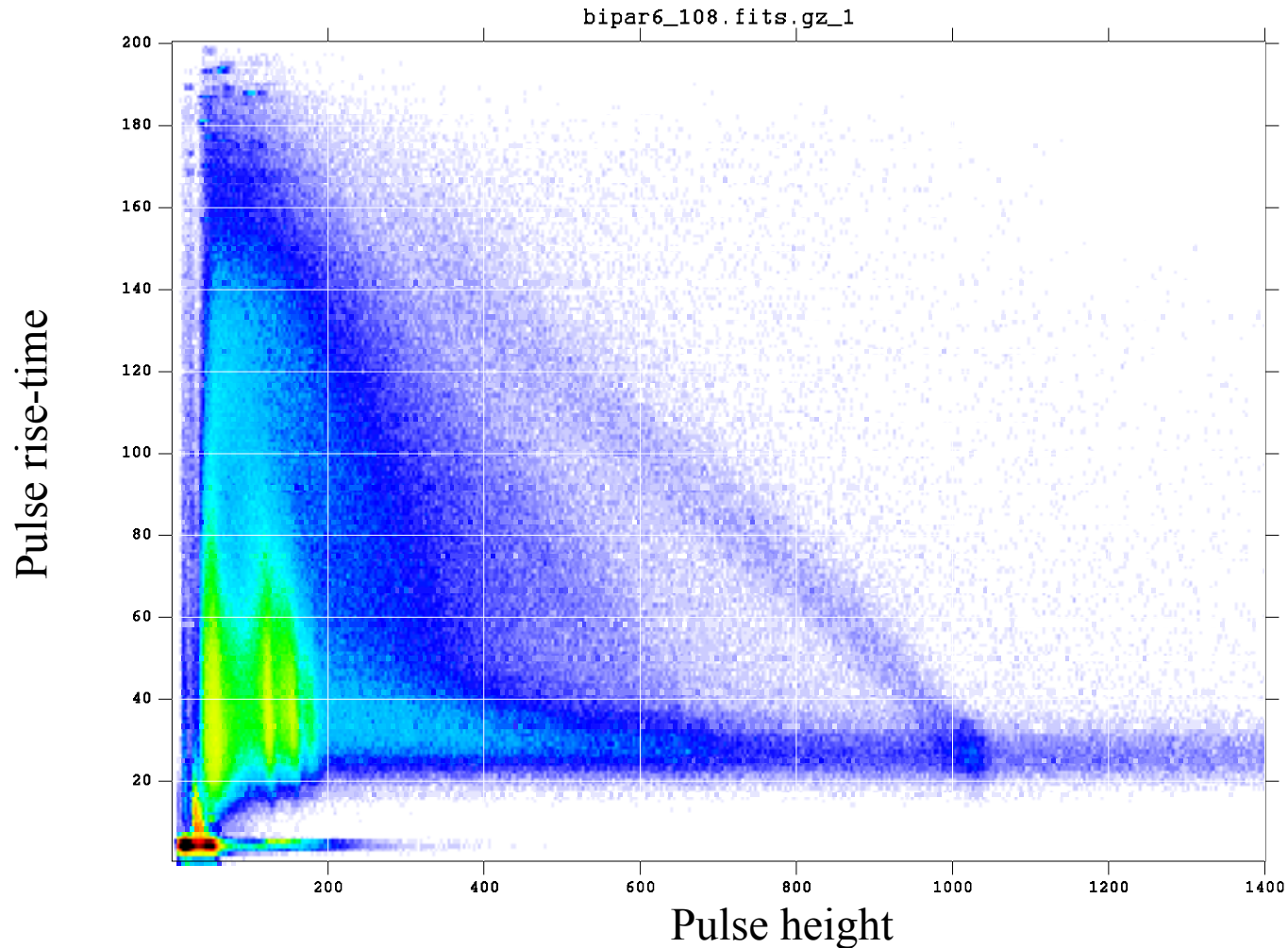


Pulse rise-time



Pulse height

Charge Loss in S2 data



ISGRI **bi-parametric diagram** showing the variation of pulse height with rise-time due charge-loss effect for in-flight data S2 (CU tagged)

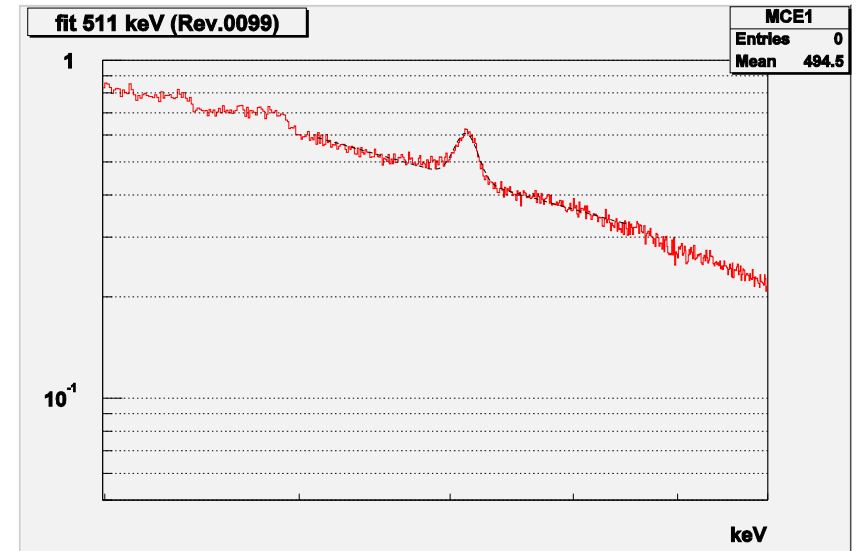
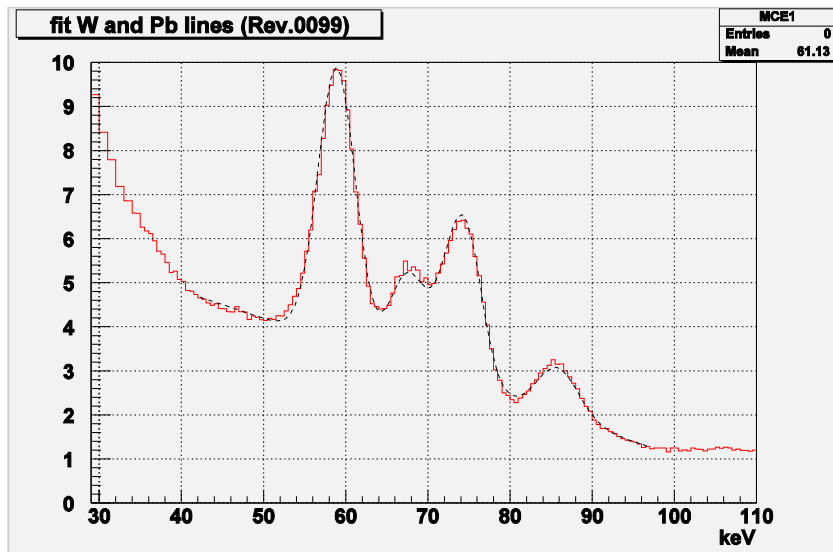
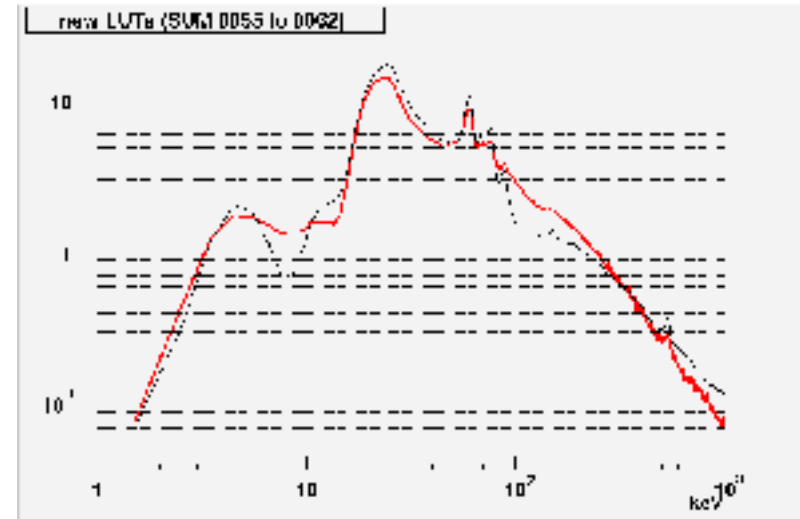
Correction of ISGRI energy

Using calibrated correction tables (Look Up Tables) an energy is computed and corrected for the charge loss effect for each recorded event.

LUT 1 used to correct for gain and offset of Pulse Height Amplitude and Rise Time

LUT 2 used to correct for the charge loss

energy in KeV is given in the COR event list



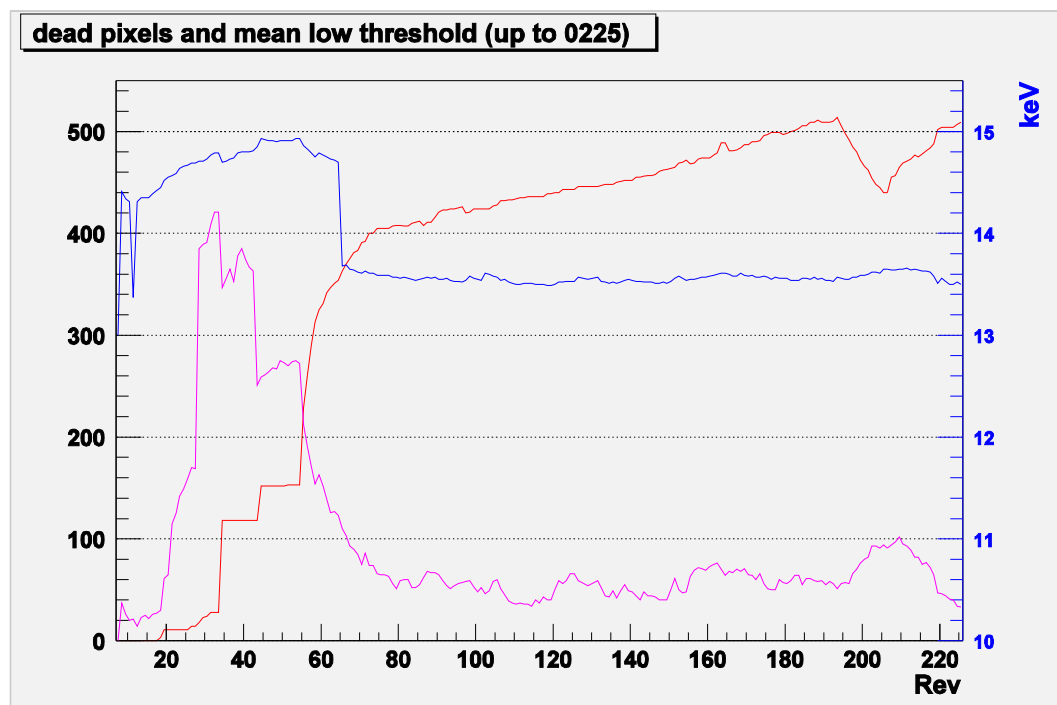
The ISGRI Noisy pixels

The ISGRI CdTe pixels are not all stable.

In spite of strong selection during manufacturing about 5% of them suffer from intrinsic noise.

An on-board s/w detects and switches OFF noisy pixels, then periodically resets them ON. The very bad ones are set off in the Context (worked out each revolution) Pixels low-energy thresholds are changed first to make them stable.

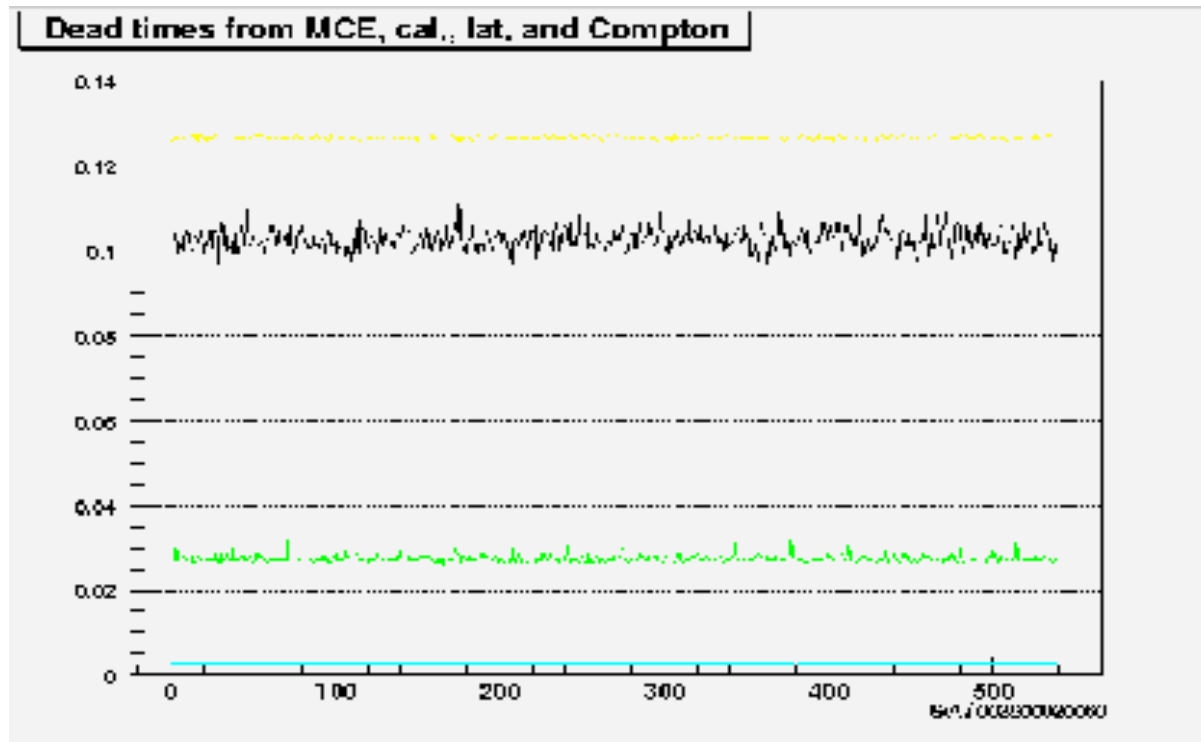
Monitoring of the instrument parameters (HK rate-meters) will provide GTI, status of pixels and dead-times



ISGRI dead-pixels and threshold evolution

- ISGRI dead pixels
- ISGRI average low-en threshold
- ISGRI max low-en threshold

Computation of ISGRI Deadtimes



ISGRI deadtimes due to different effects

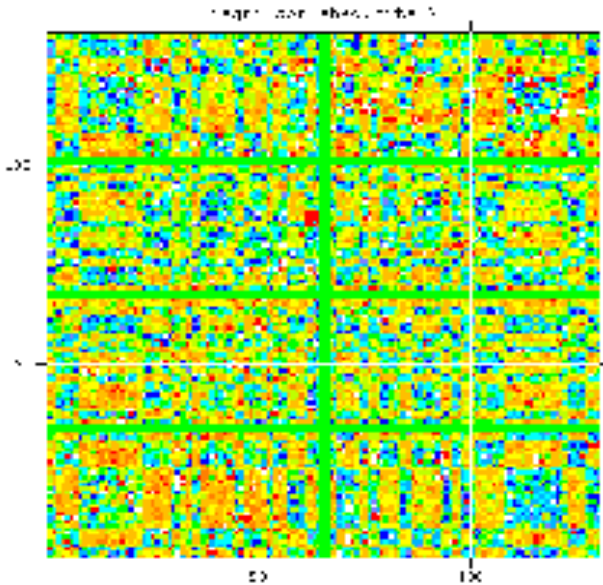
 ISGRI deadtime

 Random-coincidence Veto DT

 Random coincidence CU

 Random-coincidence Compton DT

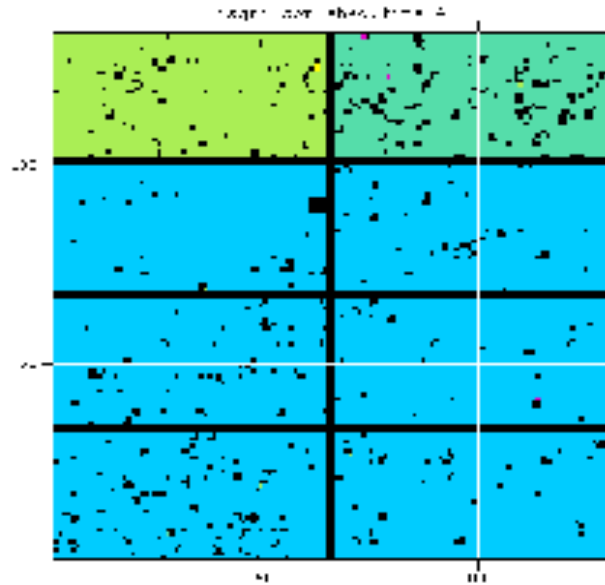
Shadow Build – Uniformity Background Correction



User GTI

Rise time bands

Energy bands



ISGRI Contexts (pixels off, low-energy thresholds)

Dead-Times (per each module)

GTIs per module

Maps of “variable” pixels off (HK3)

- Event binning in images
128 x 128 pix
- Efficiency images
- Enlarging images (dead z.)
130 x 134 pix
- Correction with Det-Unif.
& Background maps

$$\mathbf{D}' = (\mathbf{D}/\mathbf{E} - \mathbf{b}\mathbf{B}) / \mathbf{U}$$

$$\mathbf{b} = \langle \mathbf{D}/\mathbf{E} \rangle / \langle \mathbf{B} \rangle$$

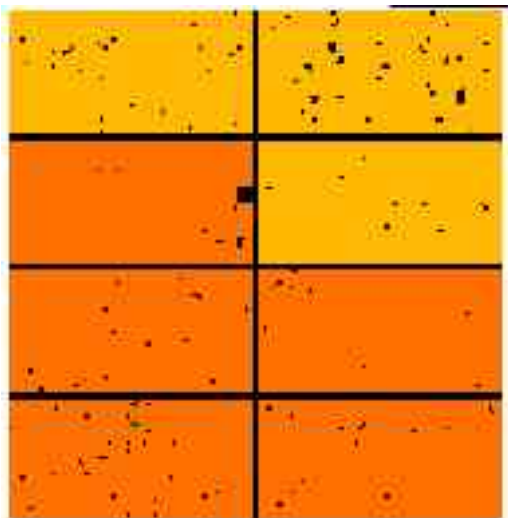
Background maps

Uniformity maps

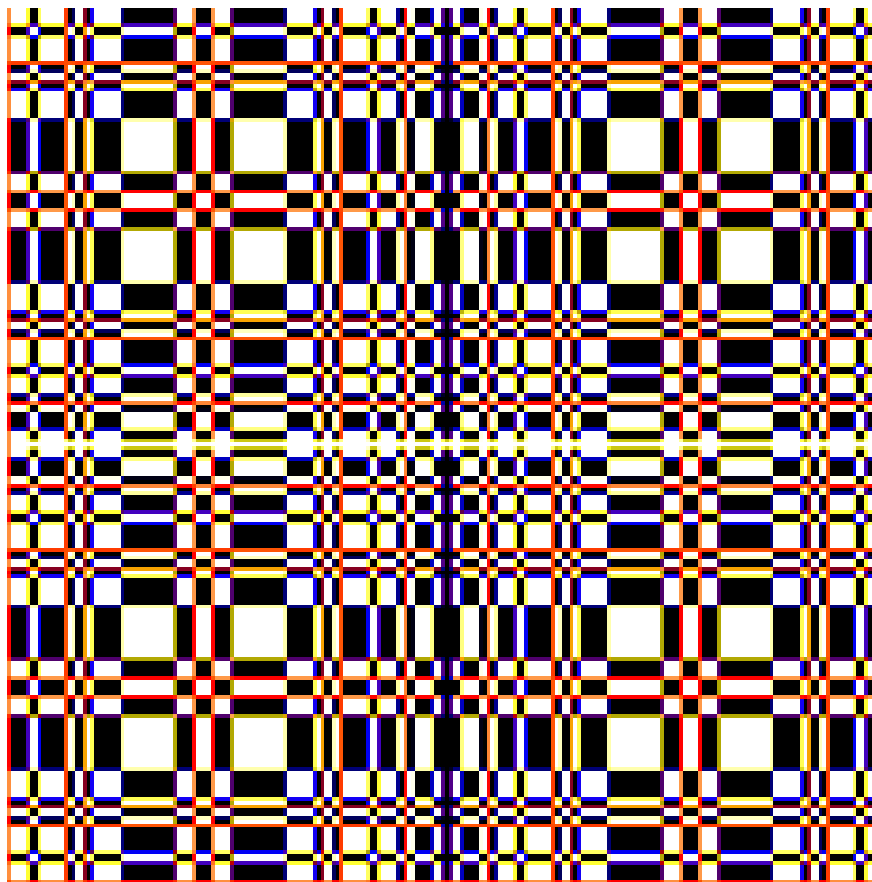
Binning to energy bands

Sky-Image reconstruction : input & decoding arrays

Decoding array obtained from the projection of the mask on the detector pixel grid (G between -1. and +1.) => a kind of "DPSF convolved" balance fine cross-correlation



D

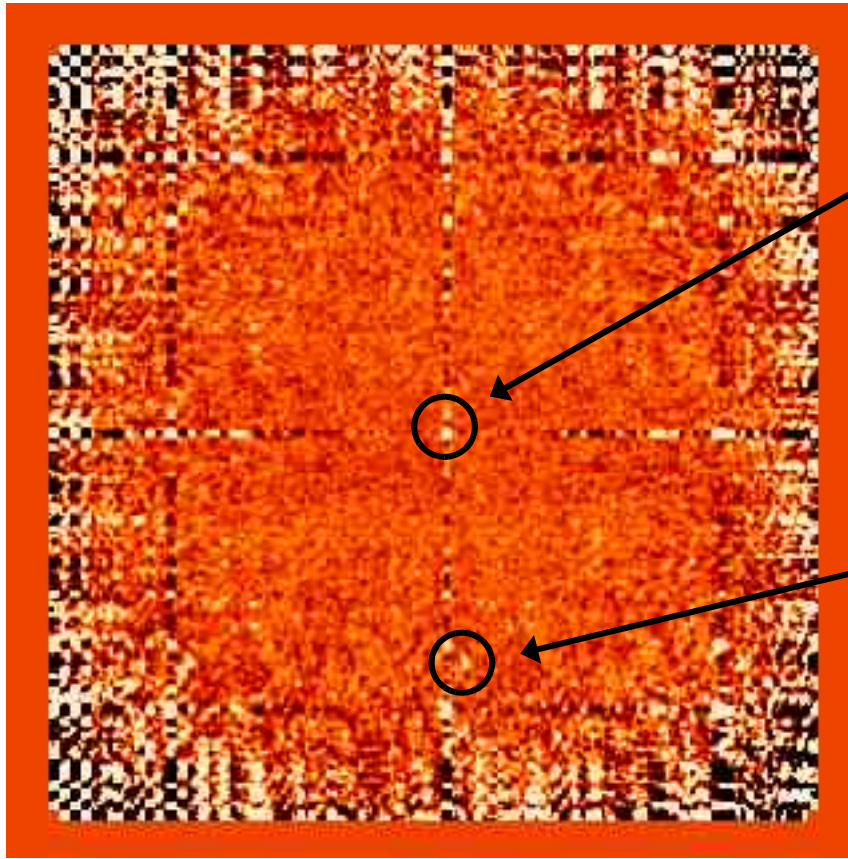


W

G

Sky-Image reconstruction : iterative procedure

Decoding: 400 x 400 pix sky maps



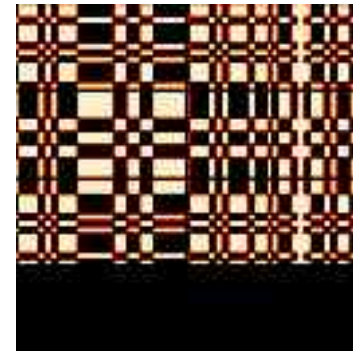
Source Detection

Excess 1
Position (SPSF fit)
Identification
Modelling →

Source Modelling



Excess 2
Position (SPSF fit)
Identification
Modelling →



Ghosts Cleaning

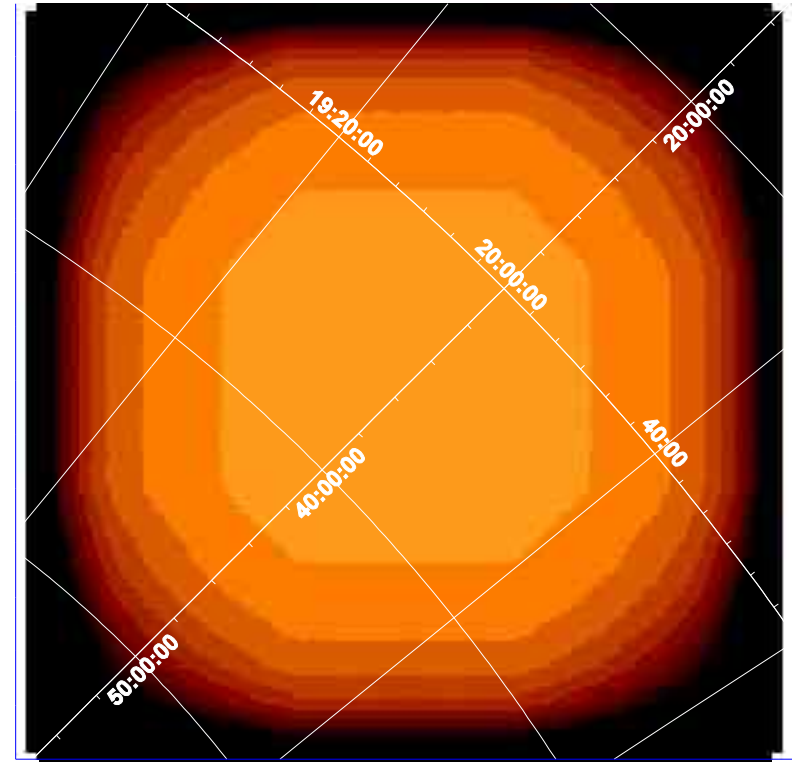
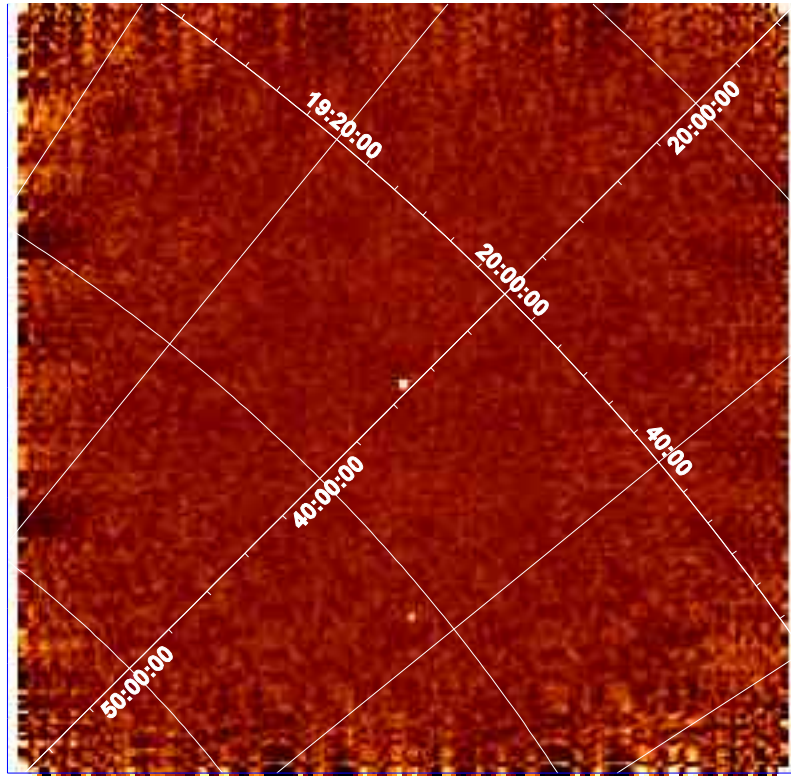
Source models are decoded, normalized and subtracted from the sky image

$$S_{ij} = \sum_{kl} W_{kl} D_{kl} G_{i+k,j+l}^+ - b_{ij} \sum_{kl} W_{kl} D_{kl} G_{i+k,j+l}^-$$

$$b_{ij} = \sum_{kl} W_{kl} G_{i+k,j+l}^+ / \sum_{kl} W_{kl} G_{i+k,j+l}^-$$

$$V_{ij} = \sum_{kl} D_{kl} (W_{kl} G_{i+k,j+l}^+)^2 + b_{ij}^2 \sum_{kl} D_{kl} (W_{kl} G_{i+k,j+l}^-)^2$$

ScW Reconstructed Sky-Images



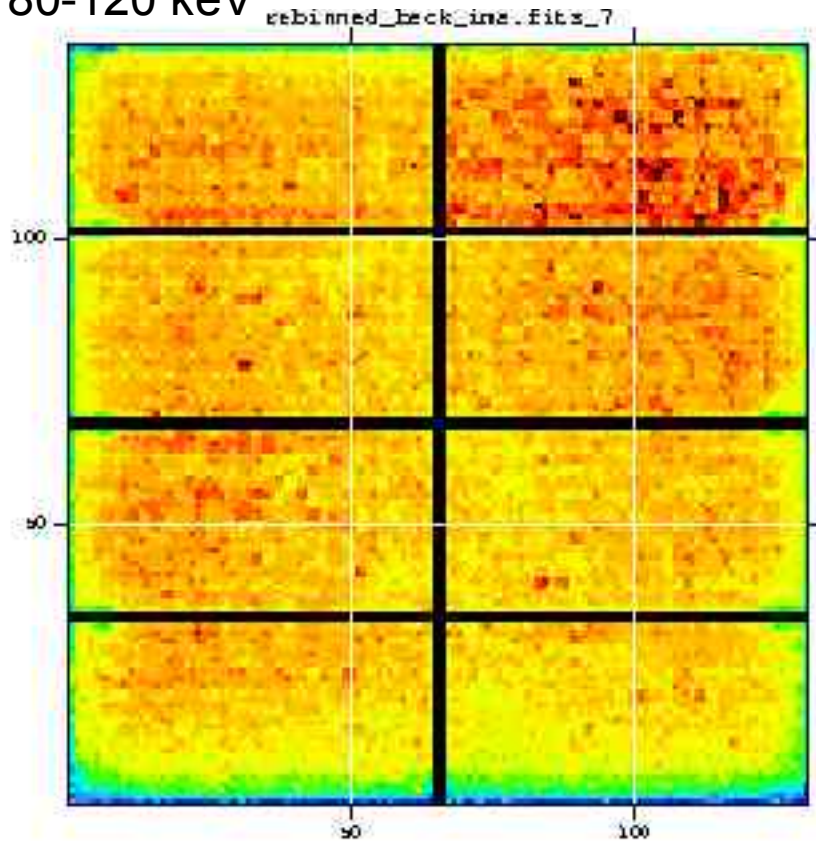
Reconstructed images (400 x 400 pix of size $\sim 5' \times 5'$) are in intensity (I) units (cts/s) renormalized to FCFOV corrected for “off-axis” effects, with variance (V) and $SNR = I / \text{SQRT}(V)$ images (+ Effective exposure and/or ghost residual images)

Parameters of “analyzed” sources are reported in output : fine position, model-flux
Flux is given by the intensity at the source pixel (**not the integral of the peak!**)

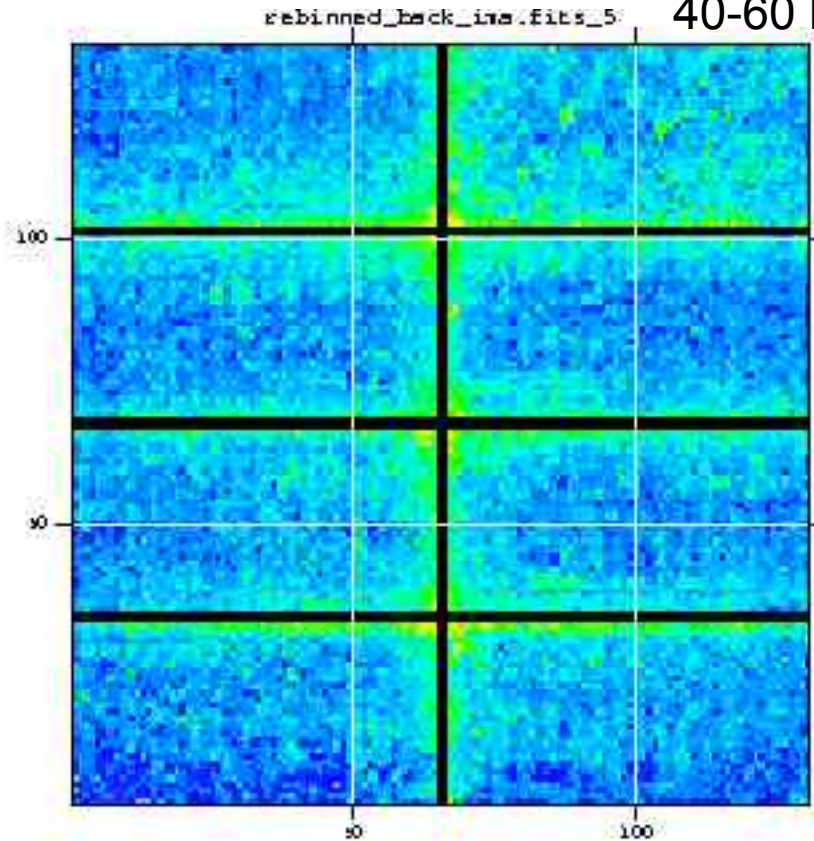
New excess must be well above 3 sigma to be really significant : rather $\sim 5-6$ sigma

Background Correction Maps

80-120 keV



40-60 keV

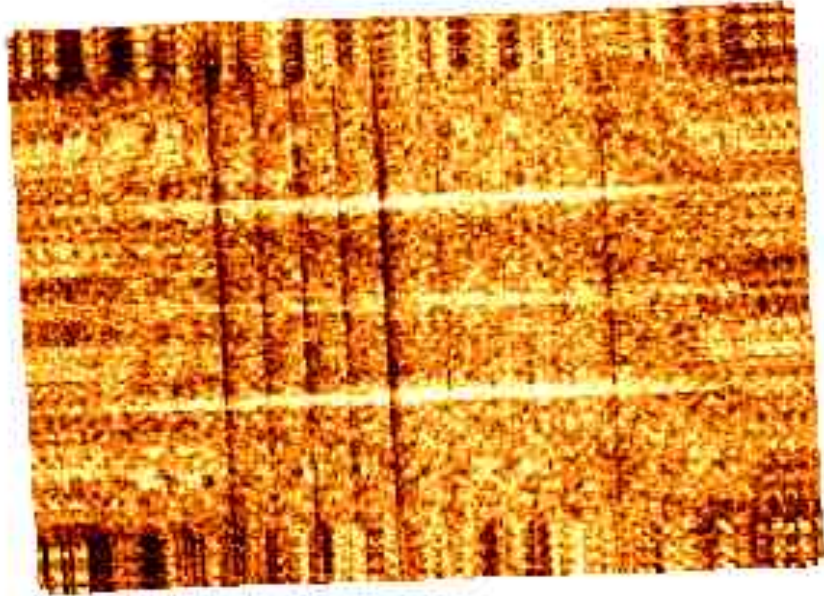


Background images are built from large sample of empty field or high latitude pointing observations. Images are corrected for efficiency.

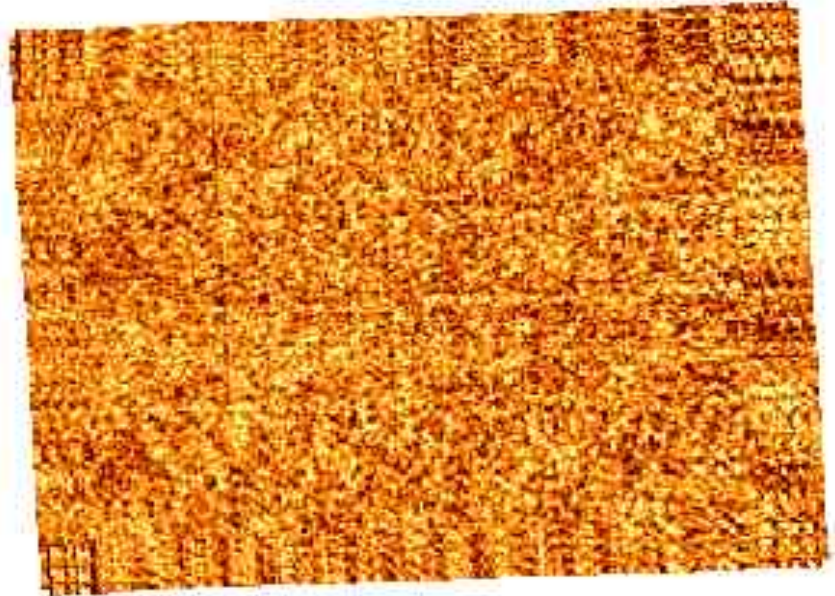
256 BKG correction shadowgrams (130 x134) for 256 energy channels.

Effect of Background Correction (100-200 keV)

un-corrected



corrected

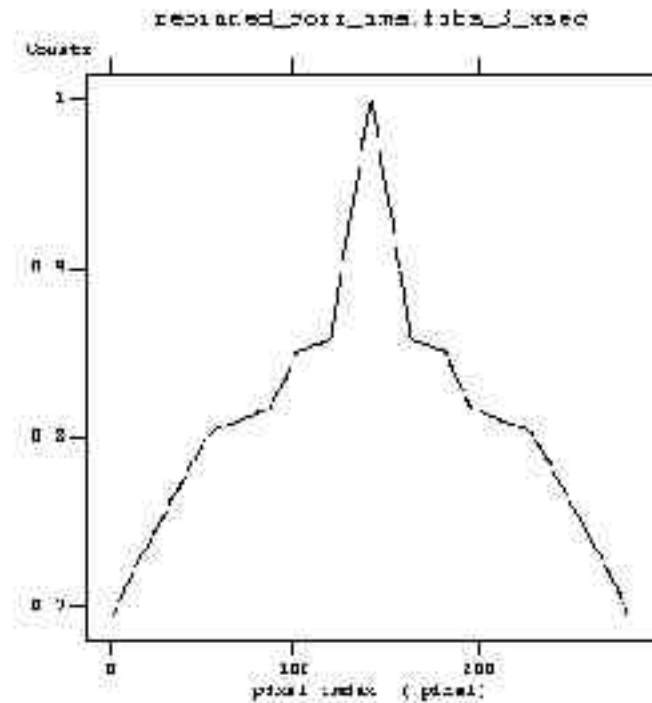
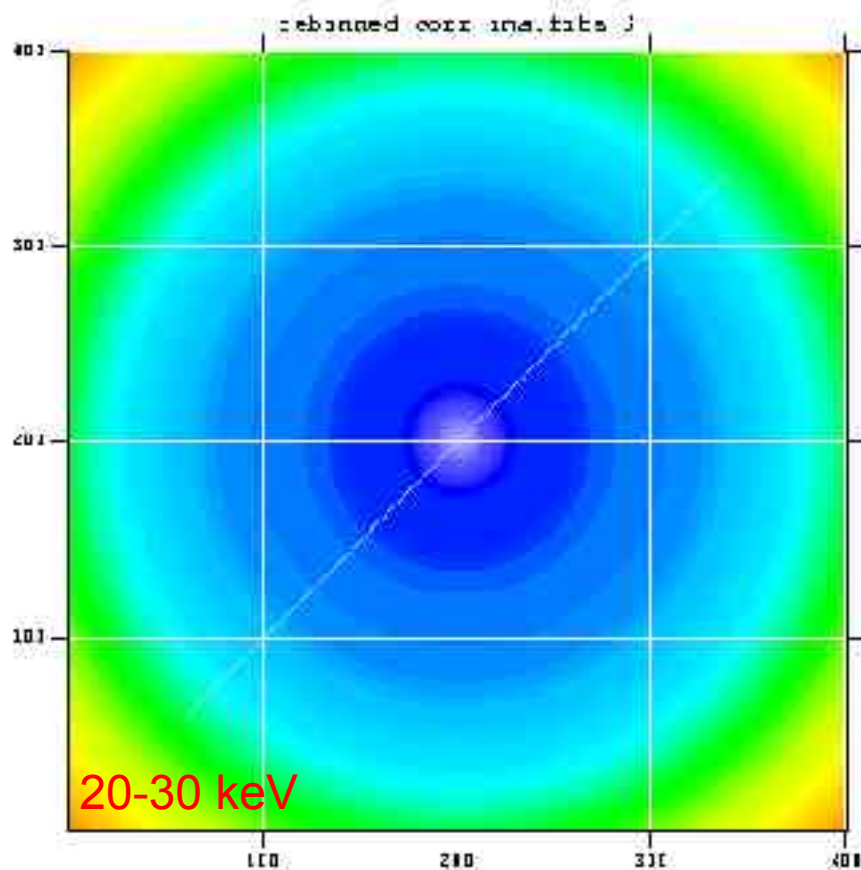


Mosaic of Galactic Center sky images (~ 5) before and after ubc correction

Some residual bkg noise present because correction maps are not perfect

One way to “measure” the “residual” bkg structures is to determine the ratio of the variance in the image to the computed variance (or look at the distribution)

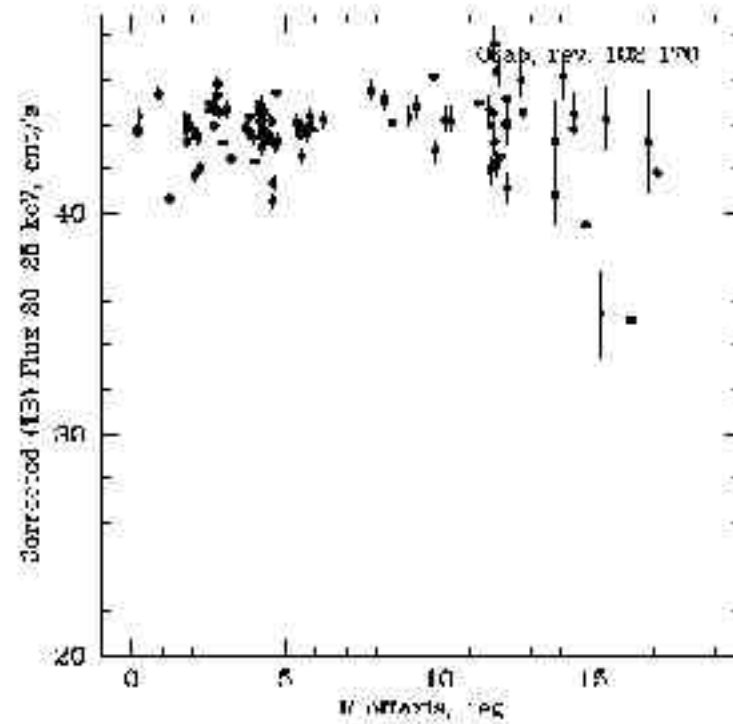
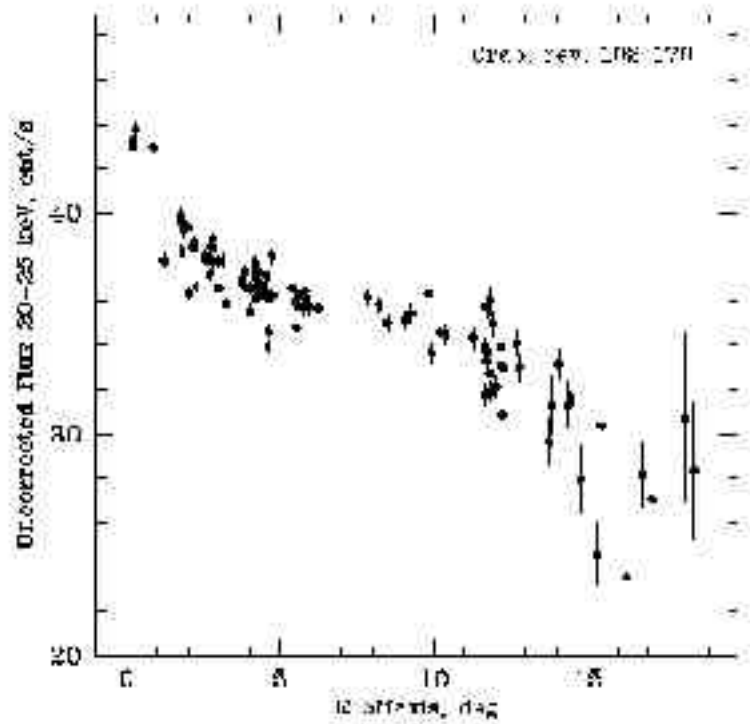
Off-Axis Correction Maps



Dependence with the off-axis position of the opacity of the mask support structure is not modeled: correction after image reconstruction

256 Off-axis correction maps (400 x 400 pix) for 256 energy channels.

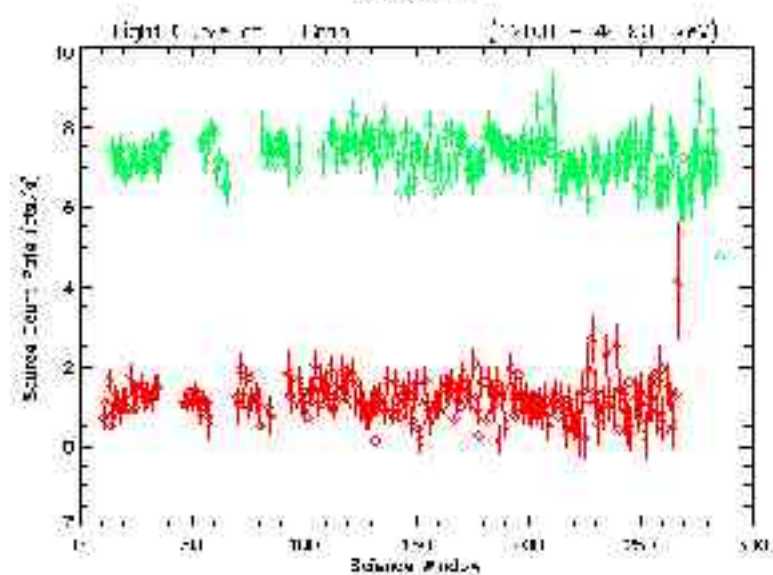
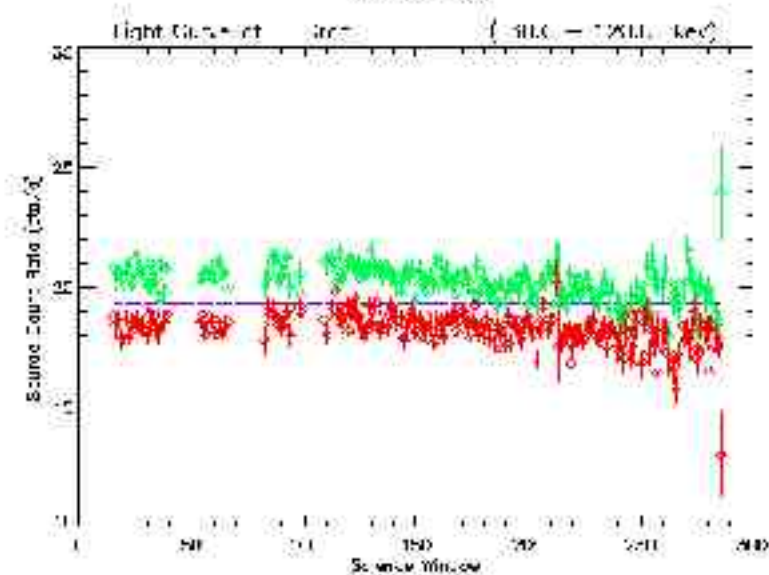
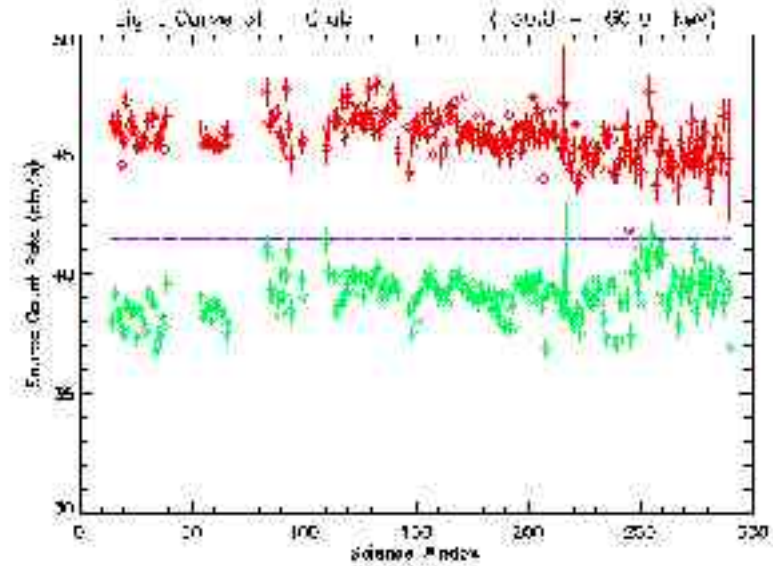
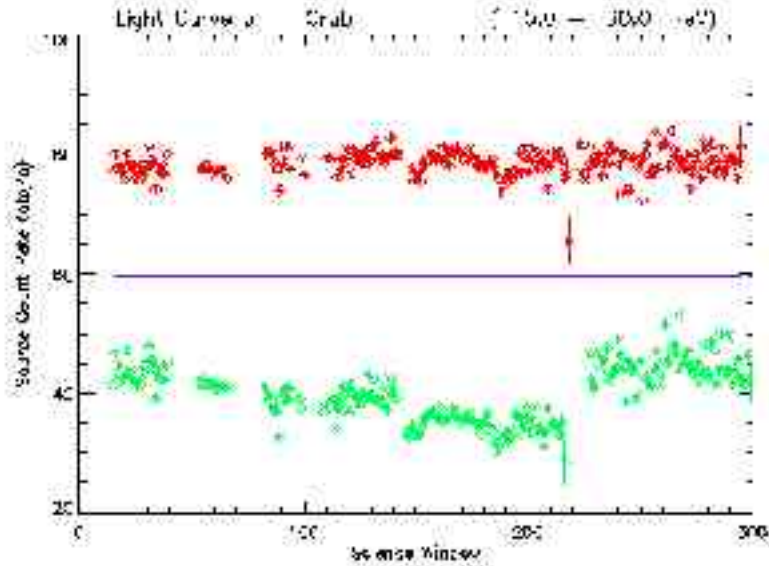
Off-Axis Correction



Dependence with the off-axis angle is corrected at the first order. Systematic scatter remains in the low energy bands due to not perfect modeling of mask support

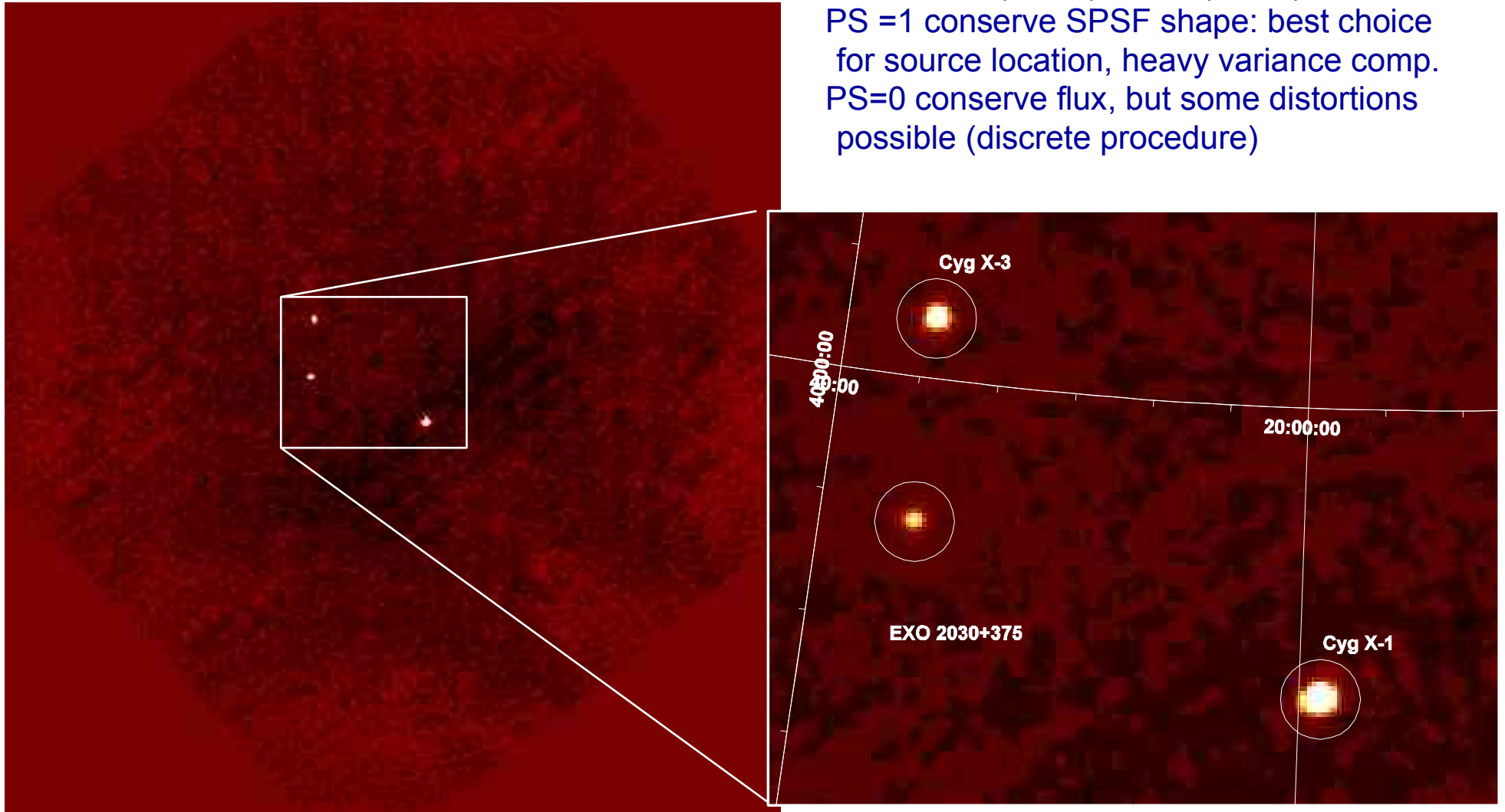
On the Crab : $\sim 4\%$ Max Dev. for 5 x 5 dithering on axis

Off-Axis Correction : Crab at $< 12^\circ$

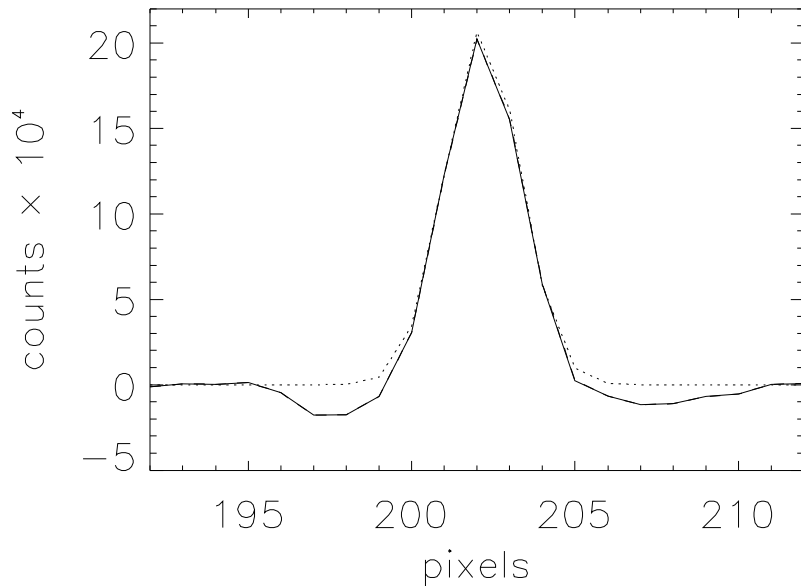


Weighted Sum of ScW Reconstructed Sky-Images in Mosaics

Two way to rotate image: pixel values are distributed (PS=1) or not (PS=0)
PS =1 conserve SPSF shape: best choice for source location, heavy variance comp.
PS=0 conserve flux, but some distortions possible (discrete procedure)



IBIS/ISGRI System Point Spread Function and Source Location



For our decoding the FCFOV SPSF (in absence of coding noise) is given by :

$$\text{[Four rectangular pulses]} * \text{[Four rectangular pulses]} * \text{[Four rectangular pulses]} * \text{[Four rectangular pulses]} \approx \mathbf{G}(w)$$

with \mathbf{G} a bidimensional Gaussian of width $w^2 = (w_M^2 + w_p^2) \sim 2.6 \text{ pix} \sim 13'$

We fit the image sector around the source peak with a function given by

$$\text{SPSF}(y,z) = I_s \mathbf{G}(y,z,y_s,z_s,w_y,w_z) + B$$

by chi-square minimization

and determine the parameters

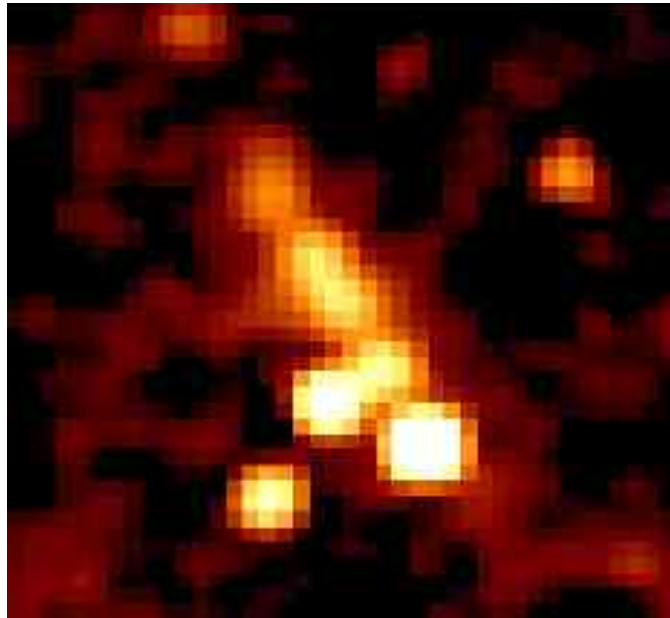
I_s = source intensity

y_s, z_s = source position

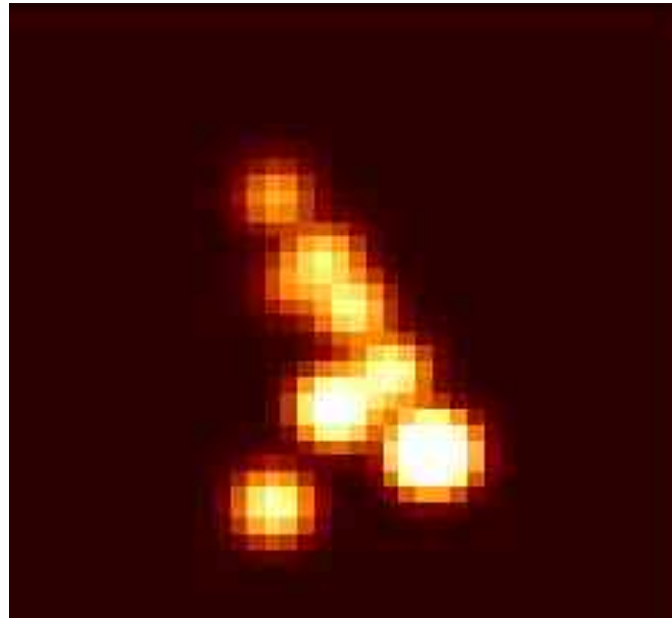
B = local background

$(w_y, w_z = \text{widths of the Gaussian})$

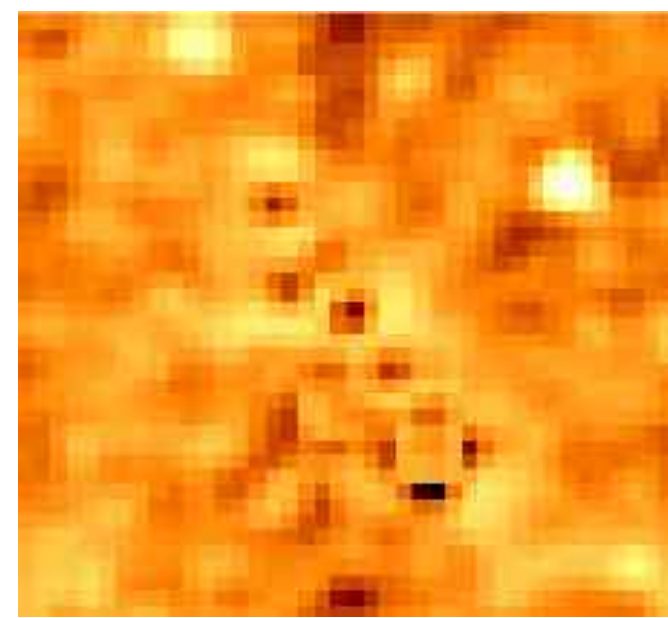
Example: Modeling IBIS/ISGRI images



Image



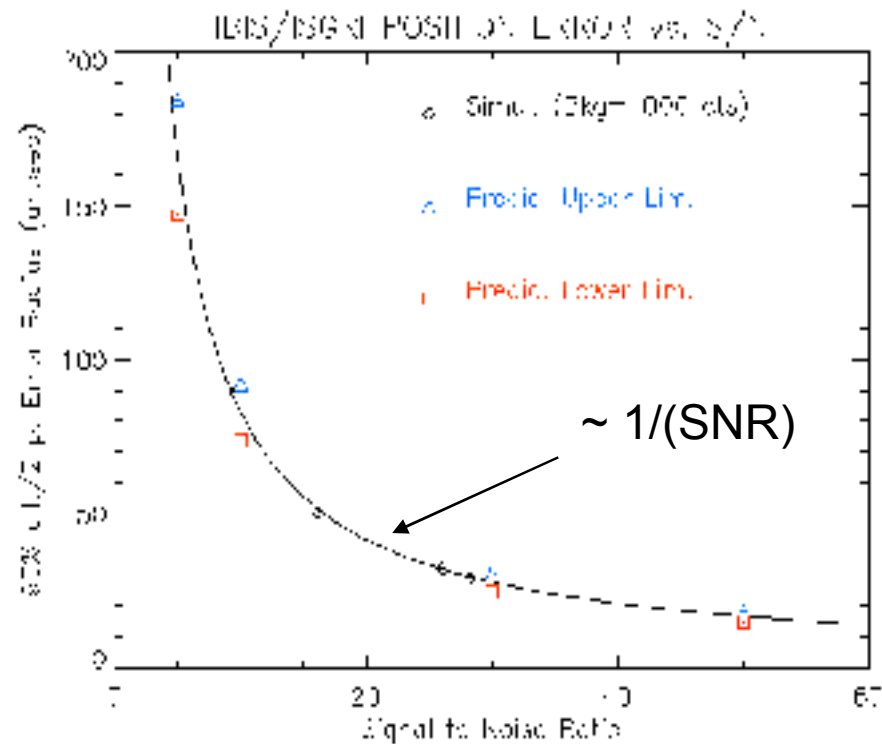
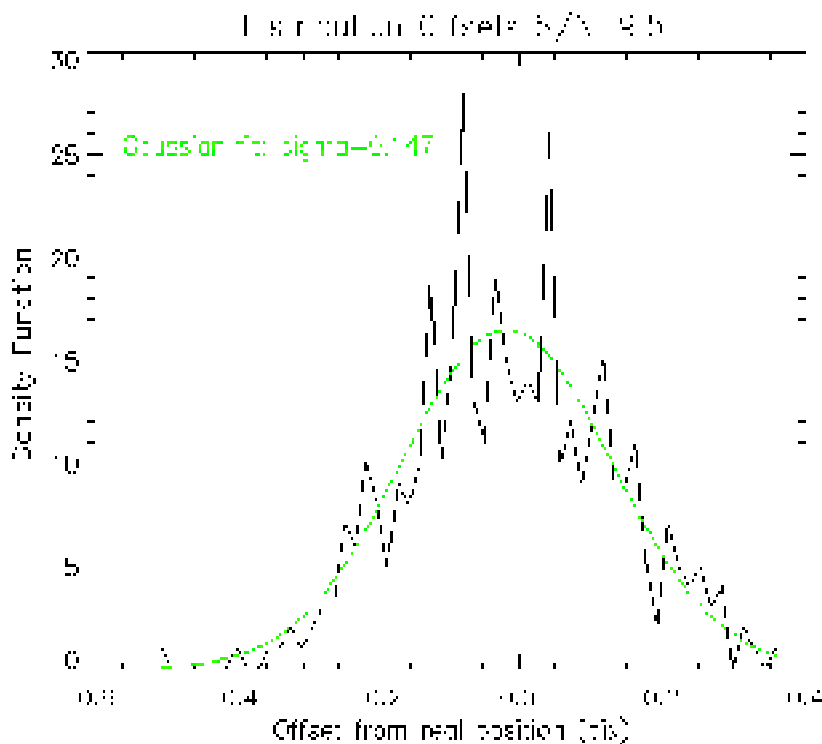
Model



Residuals

- Modeling the emission with 8 point sources (detected at least once with IBIS)
- PSF as used in the standard analysis: fit of PSF width (global parameter), source positions and intensities, and flat bkg level
- Acceptable model

Predicted IBIS Imaging Performances

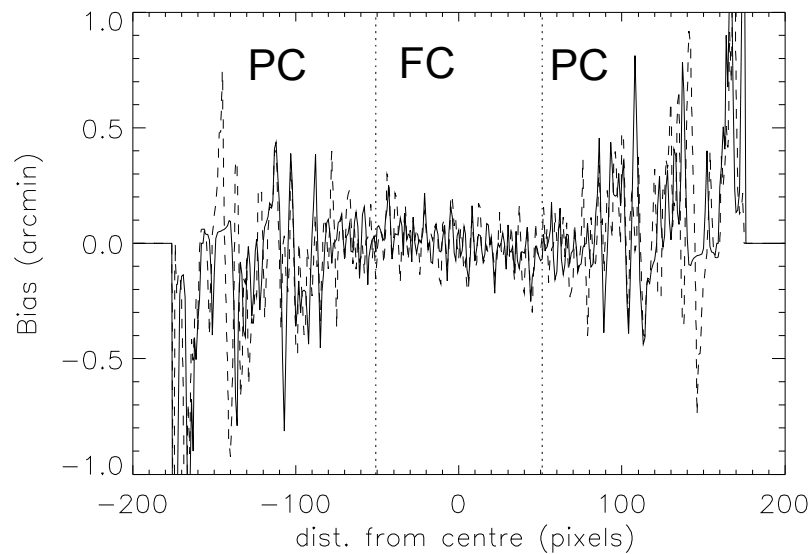
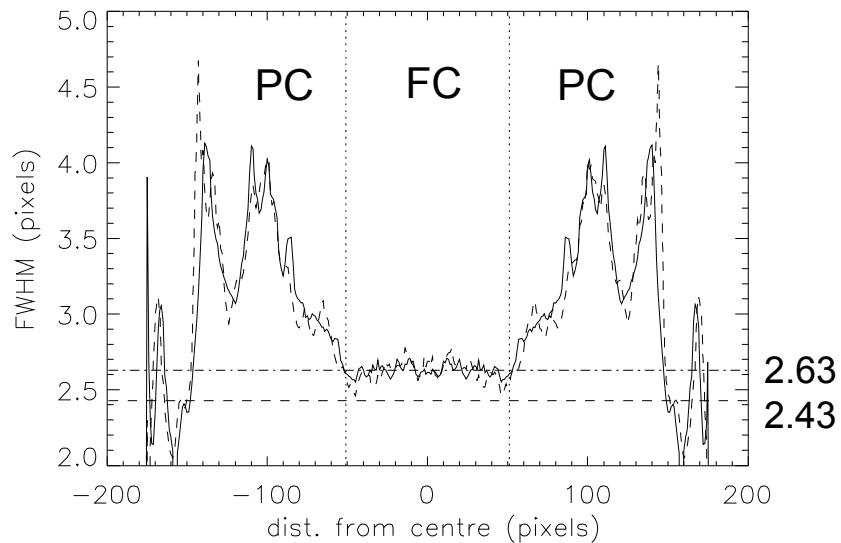
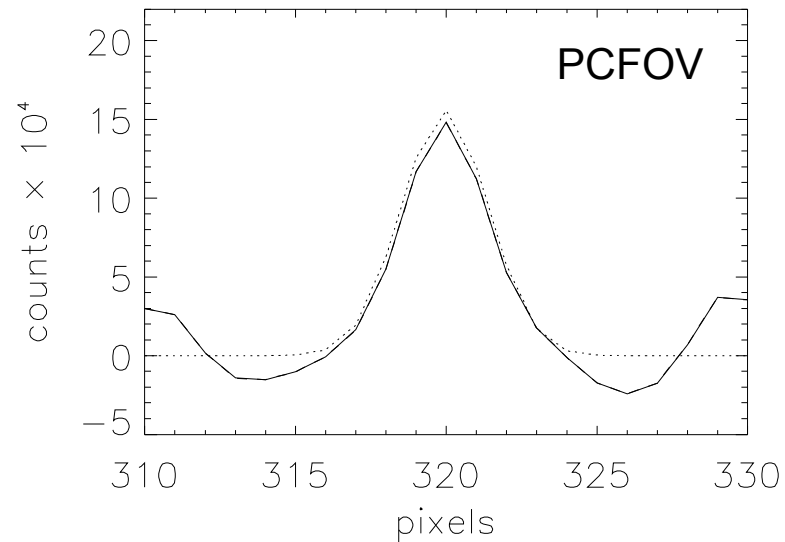
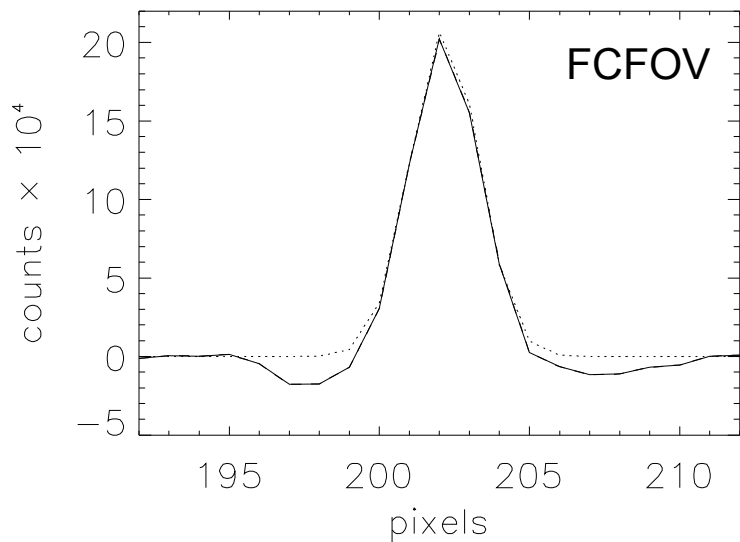


IBIS Point Source Location Accuracy

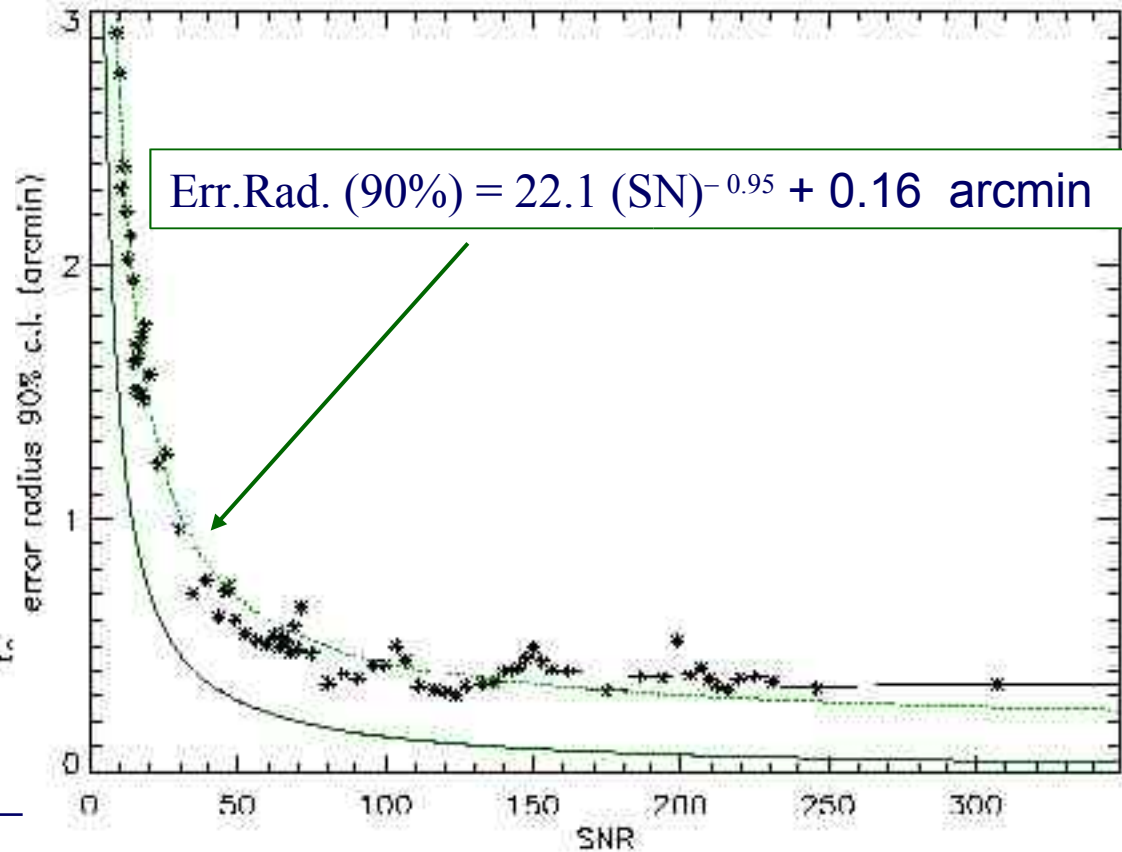
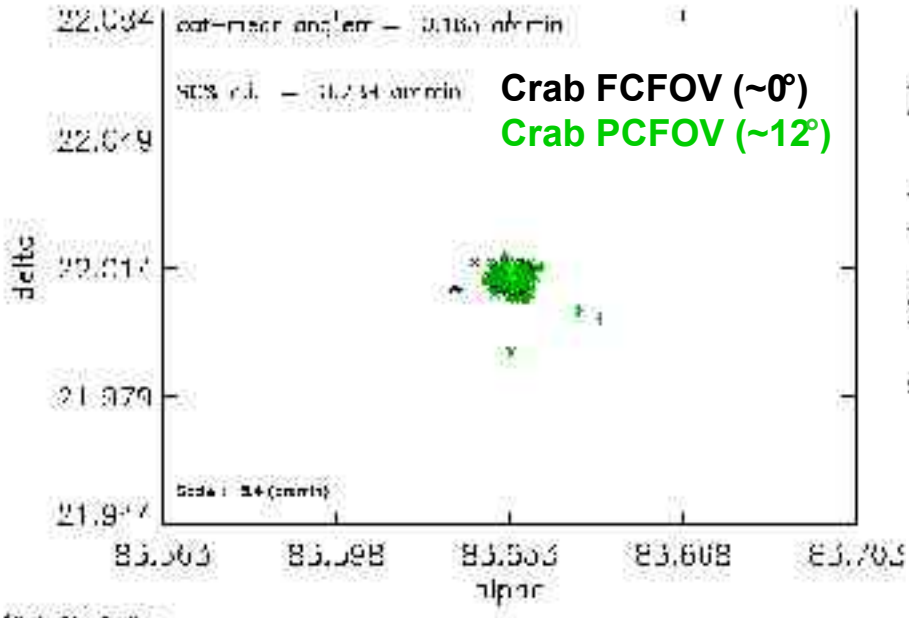
Positional error (90% c.l.) as a function of the source S/N computed using simulations for $r=2.43$ and compared to theoretical values computed for $r=1, 2$.

Positional error can be as low as $20''$ at $S/N > 40 \approx$ INTEGRAL attitude errors

IBIS/ISGRI SPSF and Source Location



ISGRI In-Flight Point Source Location Accuracy



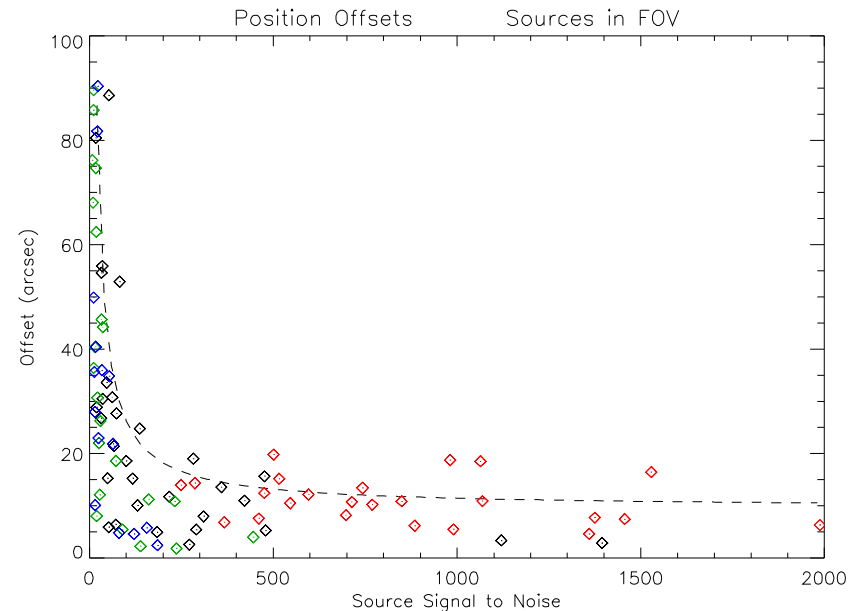
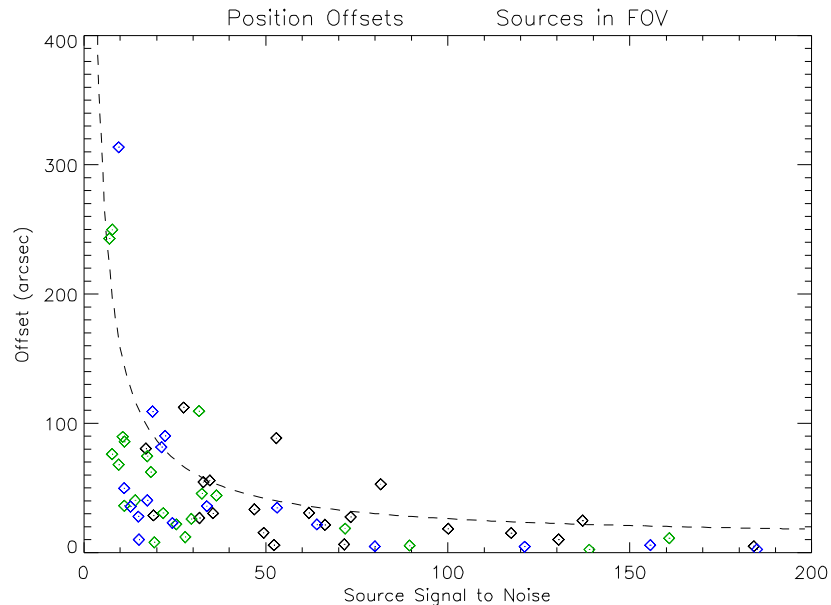
IBIS/ISGRI Source Location Accuracy

- Reconstructed positions for the Crab in FCFOV and PCFOV
- Measured 90 % confidence level radius error vs. statistical source S/N
 Data: ~ 2000 computed offsets (Crab, Cyg X-1, Cyg X-3), E ~ 20-400 keV, Axis dist. ~ 0° - 14°

Comparison with the theoretical curve (perfect system)

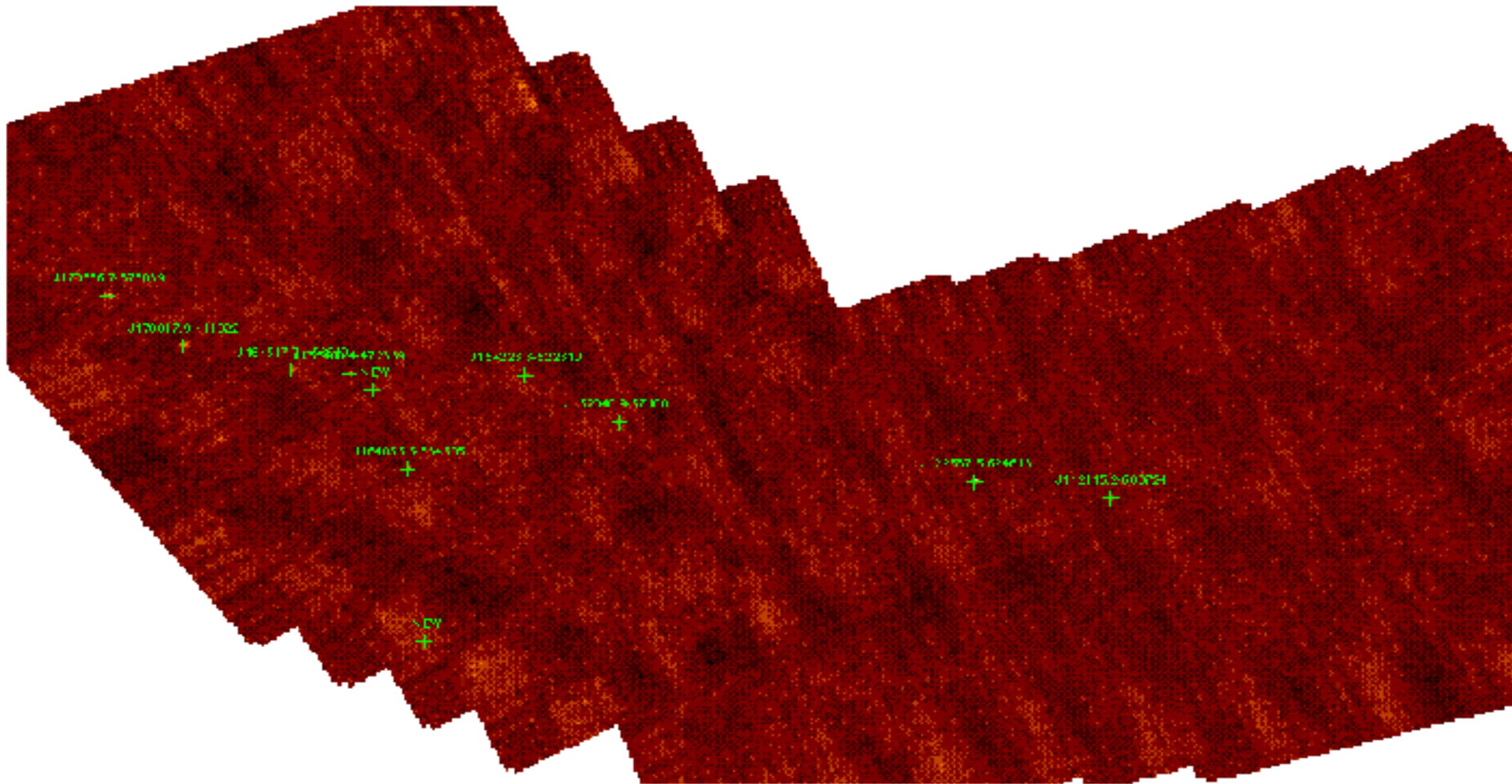
(Gros et al. 2004)

IBIS/ISGRI Point Source Location Accuracy in Mosaics

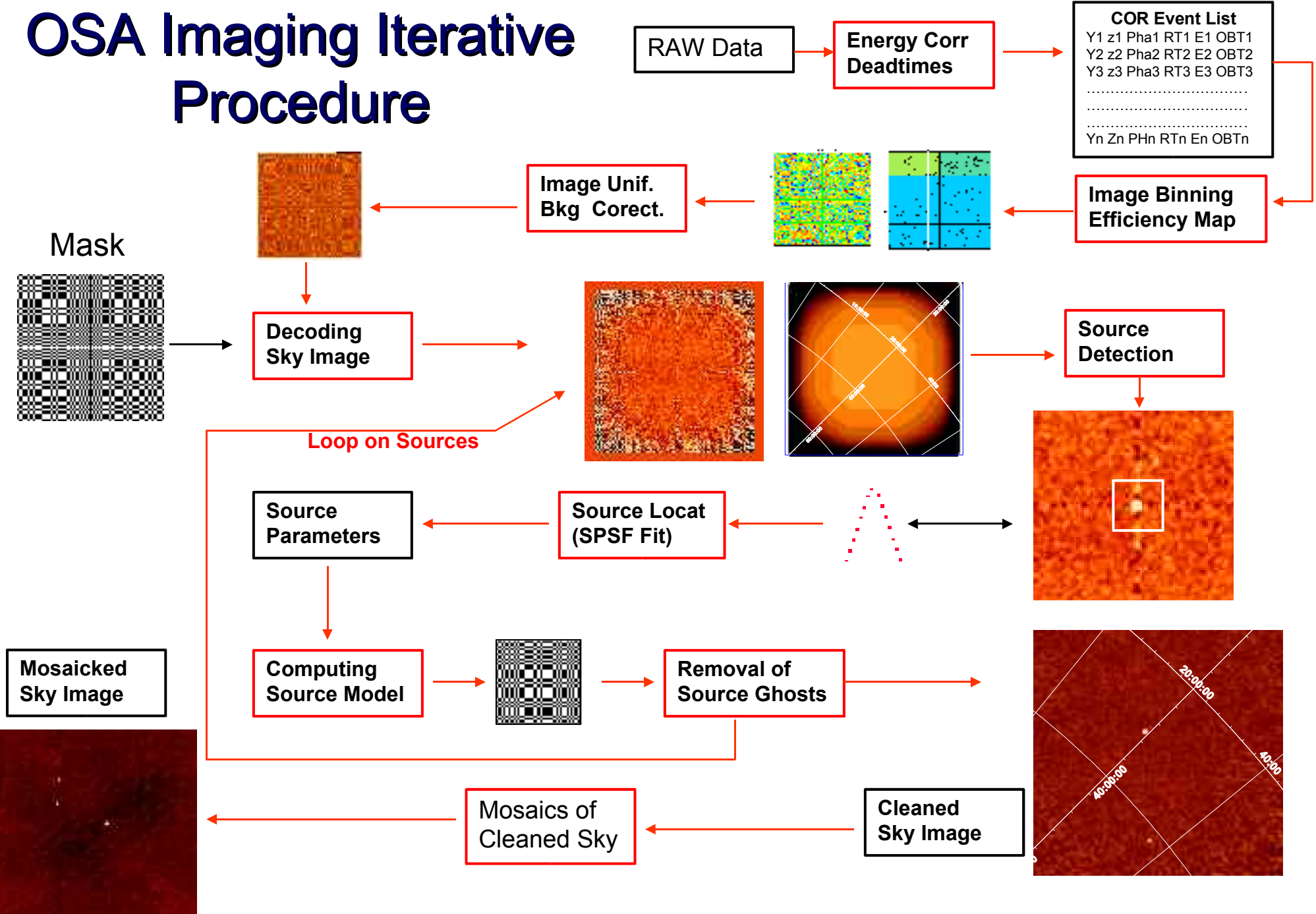


- Reconstructed positions in image mosaics for the Crab and sources in the GC
- The PSLA found for single scw images is also valid even for very high S/N in mosaics.

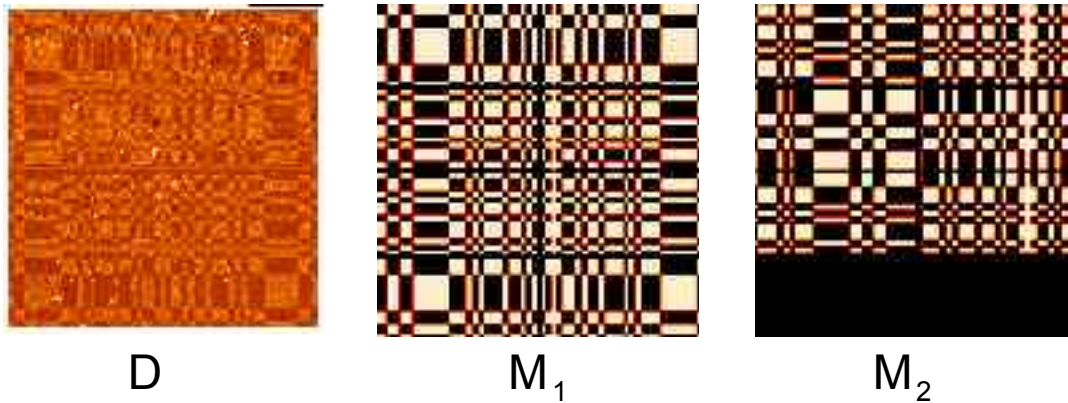
Mosaic of IBIS images from the 2nd INTEGRAL Galactic Plane Survey



OSA Imaging Iterative Procedure



IBIS/ISGRI Spectral Extraction



We can fit the detector image D with a detector model function DM including the models Ms for each active source and the Background B (including efficiency image E)

$$\mathbf{DM}(y,z,e) = \sum I_i \mathbf{M}_i(y,z,y_i,z_i,e) E + bB(e)E$$

by Least Squares or Maximum Likelihood

For each active source in the FOV of the ScW (see results of imaging) we define (for given position) a model of the source contribution in the energy band (called PIF).

and determine the parameters

I_i intensity source i ($i=1,\dots,n$)

b = background intensity

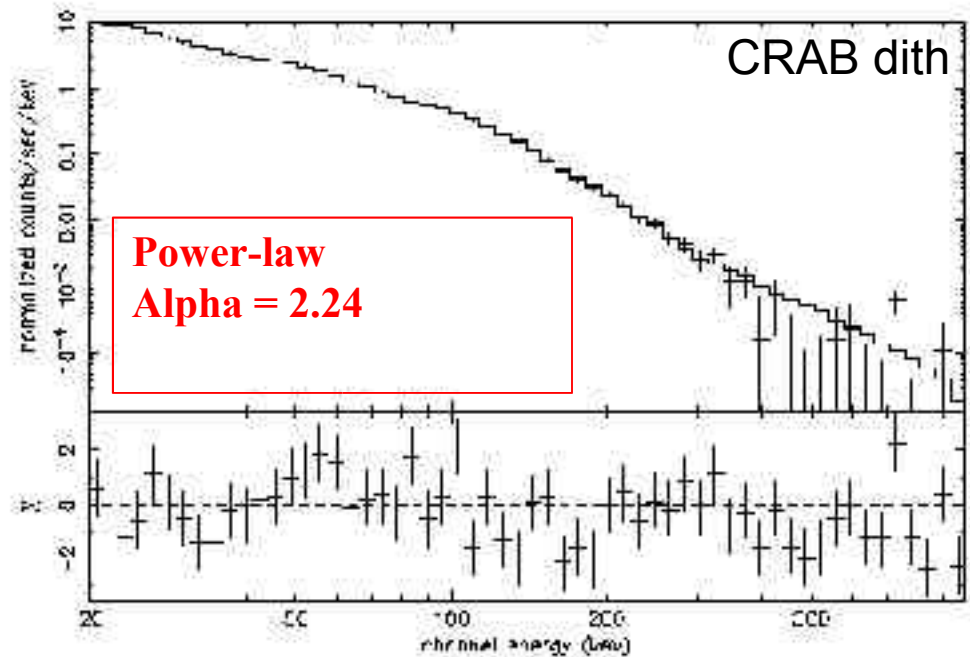
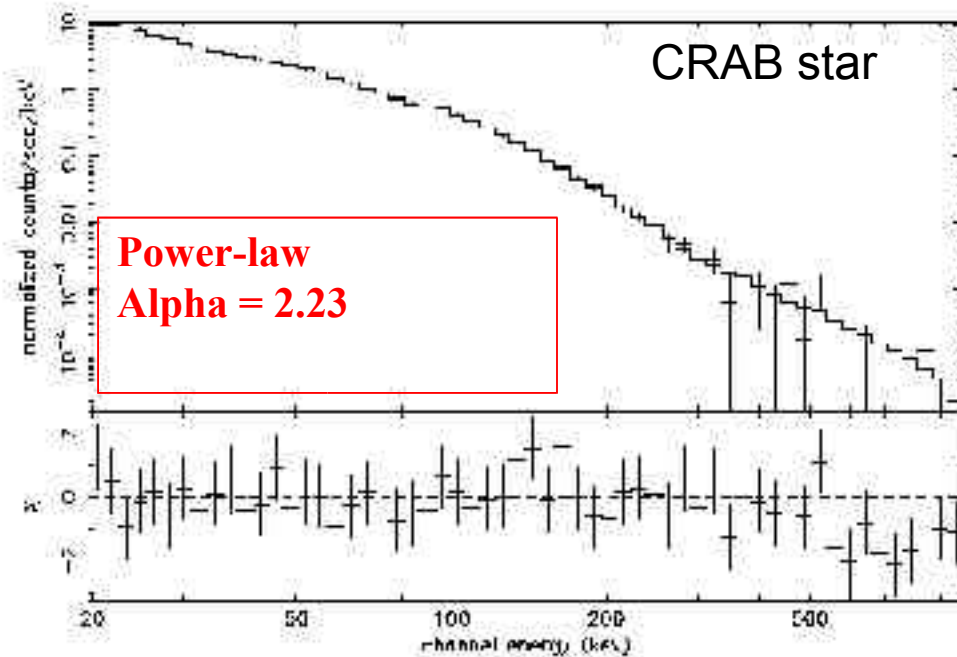
for each energy

⇒ SOURCE & BKG SPECTRA

New algorithm (default in OSA 5):

- Correct for Bkg and Eff.
- Separate fit for each source (coded a.)
- Compute contribution of each source at position of the others
- Correct first estimation from this contribution

IBIS/ISGRI Spectral Analysis

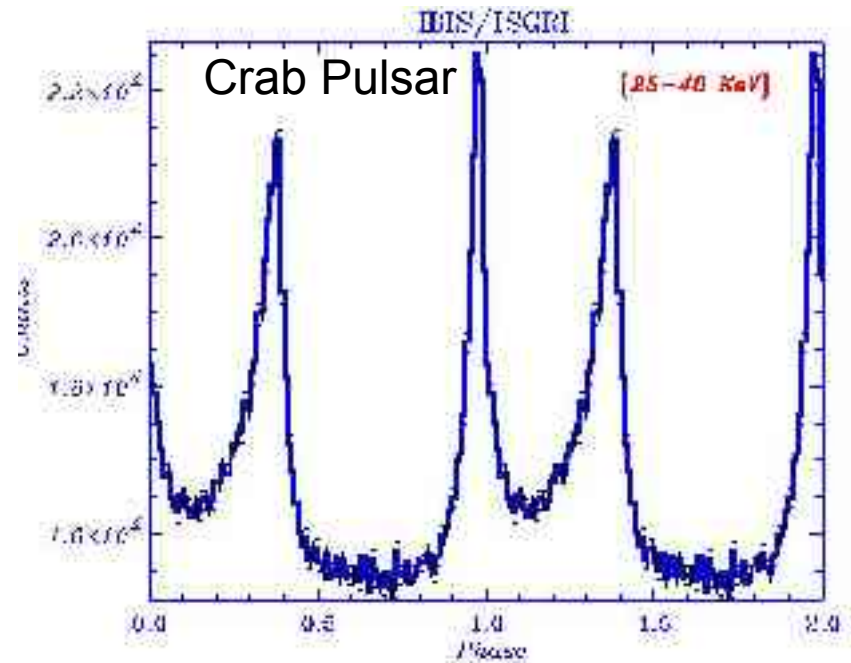
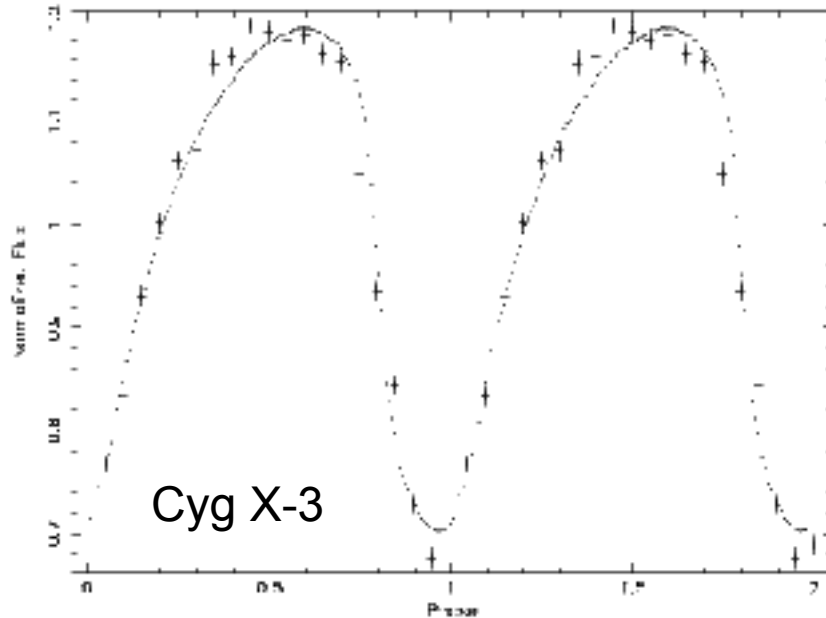


OSA 5 Crab spectrum - staring r. 102
Exp. ~20 ks – on axis – Fit 20-500 keV
Systematic required: **1 %**

OSA 5 Crab spectrum – 5 x 5 dit r. 102
Exp. ~54 ks – on ax - Fit 20-500 keV
Systematic required: **1 %**

Reconstructed spectra are compared to spectral models using Energy Response (RMF & ARF) computed from extensive Monte Carlo simulations.

IBIS/ISGRI Timing Analysis



Fluxes from image analysis provide light curves (LC) on “ScW” time-scales or longer.

See the analysis of the 4.8 h orbital modulation in Cyg X-3 (Goldoni et al. 2003)

A procedure similar to spectral extraction but applied to short time bins rather than small energy bins provides LC down to typically ~ 10 s

Photon event lists can be analysed after a Standard analysis (FFT, epoch folding, etc.) of event arrival times, possibly after appropriate selections based on the source models (PIF), can be employed for the study of rapid variability (see Crab A&A special issue)

OSA 5: new features

Low energy thresholds are more correctly taken into account in the computation of the efficiency images: increase in intensity at low energies (more compatible with expected ARF) and in S/N (because of the weighting)

Residual noisy pixels are detected before the images by tagging events (analysis of arrival times) or checking pixel total spectra (OSA 5.1)

New background and Off-axis correction images and rebinning module

New spectral extraction algorithm

Module to extract light curves (same procedure as in spectral extraction)

Module to extract the source model (PIF)

Conclusions & Recommendations

The **ISDC OSA** provides an Automatic Analysis including the described IBIS/ISGRI analysis tasks (and few other tools not described here).

The performances are “good” but careful check of results is needed:

- Check of observing conditions and scw selection: avoid solar flares, special instr. configurations, scw radiation belts entries/exit
 - Careful check of the resulting images: bad source detection/modelling, large residual bkg, energy bins at bkg lines, etc.
 - Use a proper source catalogue and source searching modes
 - Be aware of bright sources in the FOV and check ghost positions
 - Take into account the present limitations of s/w and instrument responses
 - See User Manual, IBIS/ISGRI Validation Report, known issues, other ISDC documentation and ISDC help-desk
- Please report problems (after careful check)